Experimental Insights into Partial Cation Exchange Reactions for Synthesizing Heterostructured Metal Sulfide Nanocrystals

Benjamin C. Steimle,¹ Abigail M. Fagan,^{1,†} Auston G. Butterfield,^{1,†} Robert W. Lord,¹ Connor R. McCormick,¹ Gabriella A. Di Domizio,¹ Raymond E. Schaak^{1,2,3,*}

E-mail: res20@psu.edu

Abstract

Nanocrystal cation exchange is a post-synthetic process that modifies the composition of a nanoparticle while maintaining other important characteristics, including morphology and crystal structure. Partial cation exchange reactions can be used to rationally synthesize heterostructured nanoparticles that contain two or more material segments. Increasingly complex heterostructured nanoparticles are accessible using multiple sequential cation exchange reactions, but achieving targeted structures in high yield requires careful consideration of synthetic parameters and chemical reactivity. Here, we discuss in detail the synthetic protocols used in two distinct partial cation exchange pathways that are differentiated based on the relative amounts of metal salt reagents excess vs stoichiometric - that are used during the reaction. Using a model system obtained through Zn²⁺ exchange on roxbyite copper sulfide nanorods, we demonstrate how targeted products can be synthesized reproducibly. We show how small deviations in reaction conditions, such as temperature, time, and particle concentration, can significantly impact the outcome of these reactions. We highlight important chemical and physical hazards, issues that can be encountered when characterizing heterostructured nanoparticles, and troubleshooting suggestions for overcoming commonly encountered pitfalls. Clear and detailed descriptions of these aspects of partial cation exchange reactions are important for enabling widespread reproducibly and further development of the field.

¹ Department of Chemistry, ² Department of Chemical Engineering, and ³ Materials Research Institute, The Pennsylvania State University, University Park, PA 16802

[†] These authors contributed equally

Introduction

The design and synthesis of nanoparticles that incorporate multiple materials connected through solid-state interfaces is important across many fields. Forming such heterostructures between materials with different properties has provided a means to control exciton behavior in semiconductors, create broadband absorption in a single nanostructure, synthesize photocatalysts with desired properties, develop photodiodes capable of light emission and detection, and improve thermoelectric performance. 1-8 The nanoparticle heterostructures that are envisioned for these and other applications require precise control over size, shape, composition, crystal structure, and interfaces. However, synthetic capabilities to create high-quality heterostructured nanoparticles have been significantly limited when compared to the large number of possible heterostructures that could form from combinations of even a few binary or ternary metal sulfide materials. In general, these synthetic limitations result from incompatibilities between the reaction conditions required to make different types of constituent nanoparticles – even for related metal sulfides – and these limitations often necessitate rigorous, empirical optimization of reaction conditions that are not typically generalizable. 9-11 The contrast between what researchers desire to synthesize and what they are actually able to synthesize suggests that there is a need to develop simple, generalizable, and robust synthetic pathways to create heterostructured nanoparticles in high yield.

Nanoscale cation exchange, a topotactic process that replaces cations in ionic nanocrystals while leaving the anion sublattice largely intact, is a convenient and simple post-synthetic modification strategy that can achieve many common requirements in nanoparticle synthesis, including composition, interface formation, asymmetry, and, in many cases, crystal structure. 12-14 Cation exchange has been used to transform nanoparticles that have a desired size and shape, i.e. nanoparticle templates, into a derivative product that has a different composition and therefore different properties. allowing particle morphology to be controlled independently of particle composition. 15,16 In many cases, precise crystal structure and coordination features are also conserved upon transforming the nanoparticle template to the derivative product. 17,18 This level of control allows for polymorph selectivity in an exchange product and for the synthesis of phases that are metastable in bulk systems, including some that had not been previously observed. 19-21 Synthetic control in these reactions can be expanded even further by limiting the exchange reaction so that it does not proceed to completion. Partial cation exchange provides a pathway to controllably create heterostructured nanoparticles by adding the ability to define internal interfaces within a nanoparticle.²²⁻²⁴

A variety of reaction outcomes are possible for partial cation exchange depending on conditions and product phase miscibility. Controlling time and/or quantity of the exchanging cation can produce products that incorporate a few-atomic percent dopants of the exchanged cations or those that are almost entirely exchanged, as well as intermediate amounts. Coupling these factors with consideration of the miscibility of the exchanging cations in the template nanoparticle results in the ability to form targeted products that include doped and alloyed nanoparticles, phase segregated single- or multi-segmented heterostructures, core@shell nanoparticles, and fully-exchanged systems. 12-

¹⁴ In phase segregated heterostructured products, a region with the targeted composition initiates as a reaction front (or fronts) to form one or more interface(s) within the nanoparticle template. In some systems, these interfacial regions form in specific crystallographic directions that are closely lattice matched between the template and the product crystal structure.²⁴⁻²⁷ An important aspect of partial cation exchange behavior is understanding how and why phase segregated heterostructures form and how cation exchange-based transformations can be applied rationally and sequentially to develop design guidelines that generalize cation exchange behavior and that enable the rational synthesis of complex targets.

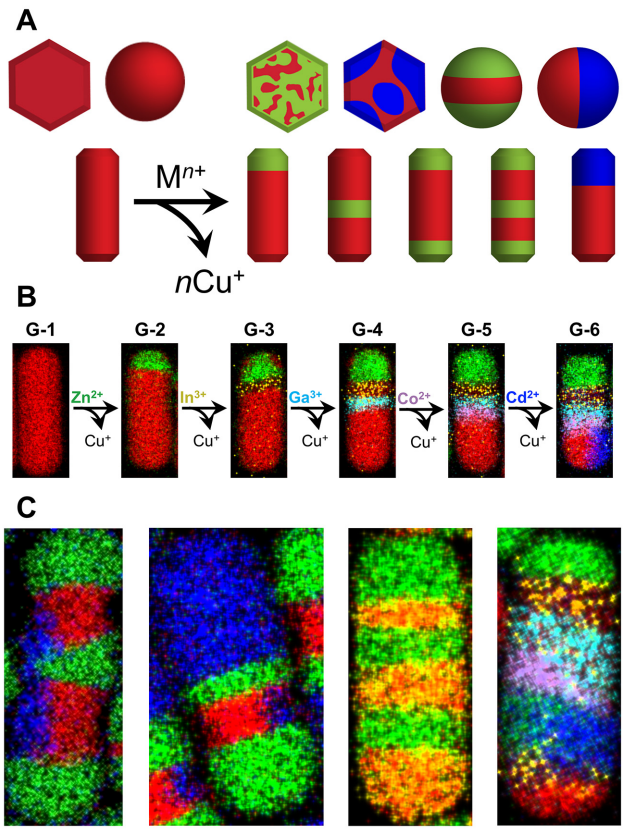


Figure 1. Possible heterostructures that can be formed through partial cation exchange reactions of roxbyite Cu_{1.8}S nanoparticles. (A) Drawings representing the range of heterostructures formed from copper sulfide spheres, rods, and plates through partial exchange Zn²⁺ and Cd²⁺. Related heterostructures formed by partial exchange with Au⁺, Co²⁺, Ni²⁺, Mn²⁺, Pd²⁺, In³⁺, Ga³⁺, and Sn⁴⁺ are also known. (B) STEM-EDS element maps showing the generational evolution of heterostructures through multiple sequential partial cation exchange reaction introduces a new region of a different metal sulfide. (C) STEM-EDS element maps of several complex heterostructures obtained through sequential partial cation exchange with up to seven individual reaction steps. Parts (B) and (C) were adapted with permission from ref. 24, copyright 2020 American Association for the Advancement of Science, and ref. 27, copyright 2018 American Chemistry Society. Cu Kα, Zn Kα, In Kα, Ga Kα, Co Kα, and Cd Lα lines are shown in red, green, yellow, teal, purple, and blue, respectively. In samples that do not contain Cd, the higher intensity In Lα line is shown.

In recent years, the synthesis of nanoparticle heterostructures has gained significant attention. As a result, recent advances have shown that tens of thousands of possible

heterostructures can be designed and potentially synthesized using multiple sequential partial cation exchange reactions.²²⁻²⁴ These phase segregated heterostructures, some of which are highly complex (Figure 1), incorporate plasmonic, semi-metallic, semiconducting, and catalytic materials that are relevant to many applications that intersect chemistry, material science, engineering, and physics. With growing interest in synthesizing and using nanoparticle heterostructures for these and other applications, rigorous methodologies must be clearly communicated. It is important to ensure that synthetic protocols, troubleshooting guidelines, detailed and characterization requirements are articulated and understood to achieve wide-ranging reproducibility. Equally important is the need for proper training and adequate evaluation of chemical and physical hazards to ensure that researchers spanning a wide range of backgrounds and experience levels have appropriate knowledge and skills. This Article will explore these considerations as they pertain to partial cation exchange reactions of copper sulfide template nanoparticles and offer insights into how to safely and reproducibly synthesize heterostructured metal sulfide nanoparticles.

Overview of Nanocrystal Cation Exchange Reactions

As mentioned above, nanocrystal cation exchange is a process that can transform a template nanoparticle into a product with a targeted composition, while maintaining key morphological and crystallographic features. The template nanoparticle is typically an ionic compound that has a rigid anion sublattice (compared to the fast time scales at which cation diffusion occurs), where both inward and outward diffusion of exchanging and template cations is possible. Cation diffusion pathways are provided by vacant cation sites, the densities of which can be modulated in some nanocrystals, and/or unoccupied interstitial lattice sites. 14 This process is solution-mediated and takes advantage of the short diffusion pathlength in nanoparticles to replace cations within a template with those from solution. Cation exchange is enabled by exploiting hard-soft acid-base (HSAB) interactions and solvation energies. 12-14 Seminal work by Alivisatos and co-workers showed that hard bases, such as alcohols, preferentially solvate harder cations, such as Cd2+ in CdSe, to help facilitate their replacement by softer cations, such as Ag+, from solution, ultimately forming Ag₂Se nanoparticles. Recovery of CdSe from Ag₂Se was also demonstrated through the use of tributylphosphine, which acts as a soft base. 15 Later work further explored soft acid-base interactions with other trialkylphosphines, and cation exchange activity was correlated with the identity of the R-groups.²⁸

The simplicity of this technique and the tunability in the chemical driving forces has created an expanding number of cations that can be used for exchange reactions on numerous nanoparticle templates, including metal chalcogenides and some metal oxides, metal phosphides, and metal halides.¹⁴ Copper chalcogenide nanocrystals are among the most widely used templates for cation exchange reactions. These phases can accommodate a relatively high density of cation vacancies, have high copper cation mobilities, and exist in many polymorphic forms with distinct structural motifs.²⁹ In particular, roxbyite copper sulfide (Cu_{1.8}S),³⁰ which can be made in a variety of shapes and sizes,²³ is highly amenable to both complete and partial cation exchange using a range of cations through preferential coordination of Cu⁺ by trioctylphosphine. For

example, complete and/or partial cation exchange has been performed on roxbyite $Cu_{1.8}S$ using Au^+ , Zn^{2+} , Cd^{2+} , Co^{2+} , Ni^{2+} , Mn^{2+} , Pd^{2+} , In^{3+} , Ga^{3+} , and $Sn^{4+}.^{20,22-25,31-33}This$ tutorial focuses on two routes to achieving partial cation exchange of roxbyite $Cu_{1.8}S$ nanorod templates with average dimensions of approx. 20×50 nm, as these systems are the most versatile reported to date in terms of accessing a large library of heterostructured systems. 24

Figure 2 shows key features of two strategies that have been implemented to create heterostructures using partial cation exchange reactions. In partial cation exchange reactions using <u>excess</u> metal salt reagents, a cation exchange solution is prepared such that the number of moles of the exchanging cations is significantly higher (*i.e.* 30-40 times in excess) than the cations in the host lattice. Different extents of exchange can be achieved by varying reaction temperature and/or time and, through empirical optimization, specific heterostructures can be synthesized. Partial cation exchange reactions using excess reagent concentrations have been used by various groups to post-synthetically modify copper sulfide templates.^{22-25,31}

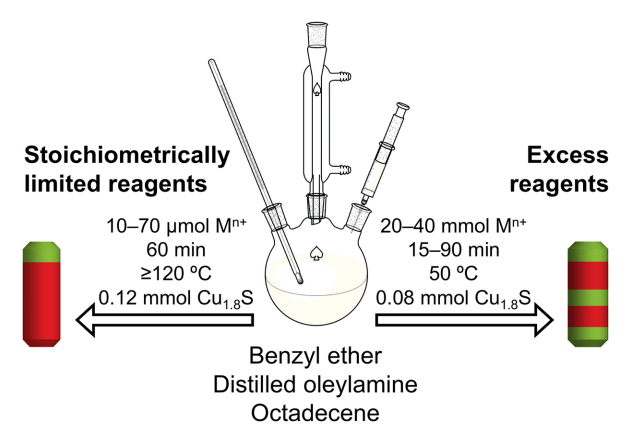


Figure 2. Overview of partial cation exchange reaction parameters for the pathways involving "stoichiometrically limited reagents" and "excess reagents". Metal salt concentration, reaction time, and temperature are different for these two processes, as are the heterostructured nanoparticles that they produce. In general, exchange with excess reagents produces multiple exchange segments, while exchange with stoichiometrically limited reagents produces fewer exchange segments. In the nanorods, the red-colored regions correspond to Cu_{1.8}S and the green-colored regions correspond to the exchanged segments.

In partial cation exchange reactions using <u>stoichiometrically limited</u> metal salt reagents, the extent of exchange is instead determined by the amount of available exchanging cations added to the reaction solution. The number of moles of cations added to the reaction flask is lower than the number of moles of cations in the nanoparticle template, making the reaction self-limiting. Performing a reaction in this way provides more direct control over the extent of exchange compared to partial exchange using excess reagent concentrations, although some empirical optimization is still required.

To successfully implement either of these cation exchange strategies to produce highquality heterostructured nanoparticles, it is important to carry out the reactions using a high degree of synthetic rigor and careful synthetic techniques. It is also important to have a complete understanding of the possible chemical and physical hazards, which may be intuitive to chemists trained in such methods but may not be intuitive for other researchers, including those who are just beginning to explore the possibility of making such particles. In addition to safety considerations, the template roxbyite Cu_{1.8}S nanoparticles can react with other components of the reaction if performed incorrectly, which results in degradation of the product. This problem is further compounded by increased reactivity in the strained regions at the interface between the newly exchanged metal sulfide and the remaining Cu_{1.8}S.²⁴ There are many variables that can combine to detrimentally impact reaction outcomes when forming heterostructures with controlled segment sizes and orientations while trying to simultaneously preserve nanoparticle size and shape.

One of the most powerful and compelling aspects of cation exchange reactions as a post-synthetic modification tool is the ability to access a variety of products using very similar reaction conditions. This capability allows us to consider a "standard" set of reaction conditions that can be slightly modified to target different products, used to troubleshoot reactions involving new cations, or develop reactions that target a specific combination of materials in heterostructured nanoparticles. Our "standard" conditions vary only slightly from one type of heterostructured nanorod to another; they have an identical reaction setup with the same ratios of solvents and surfactants combined with metal salt reagents that have a limited number of different counterions. The reagents used in these reactions each carry specific safety hazards, but consistent use of the same combinations allows for minimal changes in safety considerations between reactions. Reaction setup, general synthetic protocols, safety considerations, detailed reaction protocols, troubleshooting for each cation exchange strategy, and general troubleshooting suggestions for heterostructured nanorod formation *via* partial cation exchange are discussed below.

Reaction Setup and Techniques

Glassware and equipment. Cation exchange is a solution-based colloidal synthesis technique that typically requires air-free reaction environments and strict control over reaction temperature and time. For some cation exchange reactions and studies, reagent addition and aliquot removal are also required. These reactions can be performed using standard glassware and laboratory equipment, but several key factors must be considered when selecting these components. Glassware must be thermally resilient up to temperatures of approximately 200 °C and be capable of maintaining low internal pressures (<1 Torr) without risk of shattering; these qualifications are met by borosilicate glassware, which we use. All glassware must be free of damage such as deep scratches, star cracks, or chips and should be inspected regularly. Damaged glassware has a high risk of failure. Effective temperature monitoring and control are critical for reproducibility. Temperature is monitored using an alcohol thermometer attached to a threaded ground glass thermometer adapter. The temperature response and consistency of these thermometers are appropriate for these reactions, despite an immersion depth of only 1-2 cm in the reaction mixture. We use a glass wool heating mantle controlled with a Variac to increase reaction temperature. A tube attached to compressed air can be used to cool

reactions rapidly, if needed. Often, reaction temperatures can be more consistently maintained by wrapping the reaction vessels with insulating glass wool, aluminum foil, or another material that will retain heat. The part numbers of the glassware and equipment used by our group are shown in Table S1. A detailed description of many of these components is available in ref. 34. These reactions require standard air-free techniques and the use of a Schlenk line; several resources offer useful descriptions of detailed protocols and safety considerations, 35,36 and therefore will not be duplicated here.

Standard setup and techniques. Figure S1 shows a representative setup for a typical partial cation exchange reaction. Our generic reaction setup consists of a three-neck round bottom flask (RBF) with volumes ranging from 25-mL to 250-mL. Flasks are equipped with a condensing column, thermometer adapter, alcohol thermometer, and stir bar. In reactions that require one or more flowing inert gas steps, we use a gas-flow adapter with stopcock (Figure S1H) and place the thermometer adapter into the upper ground-glass joint. This attachment allows us to control inert gas flow while still allowing for the reaction vessel to be placed under static inert gas or dynamic vacuum and does not compromise versatility. A rubber septum is placed in the third neck of our reaction vessel to allow reagents to be injected or aliquots to be removed via syringe over the course of the reaction. The flask is connected to a Schlenk line using an angled gas-flow adapter attached to rubber or Tygon tubing. A thin layer of silicone vacuum grease is applied to all ground-glass joints to ensure an air-tight seal. All reactions require effective stirring. In practice, we stir the reaction mixture fast enough to produce a small vortex on the top of the solution without causing the stir bar to become unbalanced. In general, we use octagonal, Teflon-coated, magnetic stir bars that are 5/16" in diameter. For reaction flasks that have a volume of 100 mL or less, we use stir bars that are ½-inch in length; for 250-mL flasks, we use 1-inch long stir bars. The Teflon coating should be inspected before each use. Stir bars that have darkened in color significantly should be discarded. All glassware should be cleaned by soaking in an acid and base bath after each use, then cleaned with an alconox-based soap, rinsed with distilled or deionized water, and stored in an oven (with a temperature slightly above 100 °C) until needed.

All cation exchange reactions described here are performed using standard air-free techniques. By attaching the reaction vessel to a double gas-manifold Schlenk line, atmospheric gases and other low-boiling impurities can easily be removed from the reaction mixture through evacuation under dynamic vacuum at elevated temperature. A Schlenk line can also maintain a static or flowing inert gas atmosphere in the reaction flask. We typically use argon, although other gases, such as nitrogen, can be used. Many aspects of cation exchange reactions require manipulations of hot reaction vessels, introduction of air-free reagents via syringe, and placing reaction vessels under flowing inert gas. Those unfamiliar with proper Schlenk line techniques, air-free manipulations, and syntheses that require them should not attempt these reactions (or other colloidal nanoparticle syntheses that use similar protocols) without proper training and expertise.

Importance of maintaining a strictly air-free environment. It is important to maintain a strictly air-free environment to achieve desired outcomes during partial cation exchange reactions. Trioctylphosphine, a common Lewis base that drives cation exchange

reactions in copper chalcogenides, can react rapidly with copper sulfide in the presence of an oxidizing agent, causing dissolution of copper sulfide.³⁷ In most metal sulfide–Cu_{1.8}S heterostructures, the copper sulfide region(s) exclusively undergo this etching behavior. leaving the exchanged segment(s) untouched. This results in asymmetric dissolution of the heterostructured reaction product.^{23,37} Atmospheric oxygen can cause this dissolution reaction to occur and can be inadvertently introduced into the reaction flask through injection of various reagents or withdrawal of reaction aliquots, as is sometimes used for monitoring reaction progress. To mitigate this issue, we purge each needle and syringe prior to use for injection and aliquot removal by withdrawing and expelling Ar from a separate vessel three times before piercing the septum of the reaction flask. The higher density of Ar helps prevent atmospheric gases from diffusing back into the needle while moving between vials and reaction vessels. The transfer process should still be completed quickly after purging the needle and syringe. We also place the reaction vessel under dynamic vacuum immediately after withdrawing any needle that pierces the septum, then perform a cycling procedure with vacuum and Ar before once again placing the vessel under a blanket of Ar. These processes are used throughout the procedures outlined below and will be referred to as preparing a syringe for injection and cycling with Ar and vacuum, respectively. It is important to note, however, that if the cation exchange reaction is performed above approximately 130 °C, the cycling procedure should not be done. Doing so could cause the reaction mixture to bump, potentially contaminating the Schlenk line or damaging the vacuum pump. In reactions that require an elevated reaction temperature, it is preferable to inject the TOP/nanoparticle suspension at a temperature lower than 130 °C, perform the cycling procedure, then increase to the desired reaction temperature. This example underscores the importance of understanding all aspects of the process and the need for proper training, for both safety purposes and achieving optimal results.

Product isolation and centrifugation. Centrifugation is used to isolate colloidal nanoparticle products from suspension. We use reagent grade solvents (>99.5%) to disperse and precipitate our nanoparticle products. In this workup procedure, an antisolvent—a solvent that is miscible with the primary solvent but is not able to disperse the ligand-supported nanoparticles—is added to the solution to make the particles flocculate. In most cases, an approximately 2:1 v/v ratio of antisolvent to suspension volume produces a cloudy mixture, which is then centrifuged to isolate the nanoparticle product. Some common antisolvents used to isolate colloidal nanoparticles capped with long-chain ligands are acetone, isopropanol, ethanol, and methanol, in order of increasing polarity. Optimal antisolvents are typically identified empirically, as predicting all possible antisolvent-solvent and antisolvent-particle interactions is not straightforward. For example, we found that acetone reacts with the Co²⁺ exchange solution prepared from CoCl₂; addition of acetone as an antisolvent produces a blue, oily precipitate that is difficult to remove from the nanoparticle product. In addition to antisolvent selection, an appropriate solvent must also be chosen to re-disperse the nanoparticles after centrifugation to limit aggregation during the subsequent steps. We found that toluene, which is miscible with all four common antisolvents, works with most metal sulfide nanoparticles and cation exchange products. Other solvents, such as hexane, can be

substituted in many cases, but it is immiscible with methanol and we find that the ability of hexane to disperse as-synthesized Cu_{1.8}S is poor.

We use a Beckman Coulter Allegra X-22 centrifuge with a F0630 rotor that has six tube slots that each hold 38.5-mL centrifuge tubes, which allows us to isolate and purify full-scale reactions. We use an Eppendorf 5424 centrifuge with a FA-45-24-11, aerosol-tight rotor that holds 24 2-mL disposable centrifuge tubes to purify aliquot (< 2 mL) samples. Both centrifuges are capable of spinning to at least 13,500 RPM, which converts to 15,921 RCF for the F0630 rotor (maximum radius 78 mm) and 17,963 RCF for the FA-45-24-11 rotor (maximum radius 88 mm). Centrifugation tubes should be tightly closed, properly balanced, and not overfilled, i.e. typically ~¾ full as a maximum amount. All tubes, especially those that are reusable, should be inspected for damage prior to use.

Safety Considerations

It is important to be mindful of chemical safety and proper handling of nanomaterials in all aspects of colloidal nanoparticle syntheses.³⁸⁻⁴² First and foremost are the hazards specific to the reagents used in these reactions. Many of the metal salt reagents are respiratory irritants and some, especially those containing cadmium or cobalt and the phosphine-based decomposition products of TOP and related phosphorus compounds, are highly toxic. Many of the other reagents used in these reactions are also respiratory irritants, acutely toxic, and/or corrosive. Detailed safety considerations for each chemical can be found in safety data sheets (SDS), available through most chemical supplier webpages. The SDS for each reagent should be reviewed, and proper precautions taken. prior to performing any colloidal synthesis reactions. Standard personal protective equipment (PPE) such as nitrile gloves, safety goggles or safety glasses with side shields, and chemically resistant lab coats are necessities when performing cation exchange reactions. Additionally, engineering-based protections, such as the proper use of a chemical fume hood during reagent and reaction product transfer steps, are critically important to prevent accidental chemical exposure. For all discussions of synthetic protocols below, we are assuming proficiency in air-free synthesis, handling of colloidal nanoparticles, and Schlenk line use. As for any chemical reaction, individuals that implement these techniques without proper knowledge, training, and proficiency place themselves and those around them in danger.

Handling toxic metal salt reagents. Metal salt reagents are used in the synthesis of template nanoparticles and in the preparation of cation exchange solutions. Many metal salts are toxic and corrosive, including through contact and inhalation of dust or particles. In addition to the "standard" PPE (lab coat, goggles, nitrile gloves), researchers should consider using a filtering respirator certified by the National Institute of Occupational Safety and Health (NIOSH). The reagent-specific SDS will indicate the NIOSH classification (e.g. N-95, R-95, P-95, N-99, etc.) of respirator suggested for safe handling. At a minimum, we recommend using respirators that are classified as N-99, which filter out at least 99% of non-oil particulates, when handling most metal salt reagents. Researchers should exercise extreme caution when using reagents that contain cadmium

and cobalt, as they are extremely toxic and carcinogenic, and can lead to organ and/or reproductive damage. Other salts, including ZnCl₂, MnCl₂, and InCl₃, are also classified as toxic, corrosive, and/or irritants with significant negative health effects if handled improperly.

Alkylthiol reagents. Alkylthiols are used in the synthesis of metal sulfide nanoparticles. 1-dodecanethiol and *tert*-dodecanethiol are common reagents that are corrosive and can cause irritation and serious damage to skin and eyes. These reagents typically have a strong, nauseating odor. Special care must be taken when handling these reagents, and they should never be opened outside of a chemical fume food. Reactions that use these reagents should be worked up entirely in a chemical fume hood and transferred carefully to centrifuge tubes with tight-fitting caps before being moved to a centrifuge. Spills should be cleaned quickly, and contaminated gloves removed and replaced immediately. All reaction components (glassware, centrifuge tubes and caps, etc.) that contact alkylthiols should be first rinsed with isopropanol, then with an aqueous bleach solution (1:1 mixture of commercial bleach and water).

Solvents and other reagents. Several high-boiling point solvents and surfactants are used in partial cation exchange reactions. Benzyl ether, the primary solvent in partial cation exchange reactions, is classified as an acute, single exposure inhalation hazard. This reagent should not be stored for longer than three months because it has the potential to form organic peroxides, much like other ethers. It should by tightly closed when not in use. Oleylamine is both a solvent and a surfactant. It is highly corrosive and causes serious skin and eye damage. Octadecene is used as a solvent in the synthesis of template nanoparticles and in partial cation exchange reactions. It is a viscous liquid that can be fatal if inhaled or swallowed. Any spills of these chemicals should be cleaned up immediately and completely; a film of oleylamine or octadecene on a bench top can be just as dangerous as if it was spilled on a glove or lab coat. Contaminated gloves or other articles of PPE/clothing should be removed immediately and disposed of safely. Most of the solvents used in these syntheses have high boiling points that provide access to the high temperatures required for the formation of nanoparticles and cation exchange precursor solutions. However, exposing these solvents to vacuum during degassing steps can significantly lower their boiling points. Because of this, we generally do not exceed temperatures of 130 °C when heating under vacuum to avoid pulling the reaction solution into the Schlenk line. Hexanes and toluene are commonly used to suspend nanoparticles for storage. These reagents are neurotoxic and should be used and stored in a fume hood to avoid inhalation.

Handling powdered nanoparticles. Powders of nanocrystalline solids pose a significant risk to researchers. The health effects of many nanomaterials are not fully understood and exposure to any of these materials should be avoided. Although the ligand-capped roxbyite Cu_{1.8}S nanorods typically form macroscale aggregates when dried, they still should be handled with extreme caution and treated as serious inhalation and contact hazards. The specific hazards of this process should be evaluated prior to drying a nanoparticle suspension. These hazards must be evaluated for each nanomaterial. The best way to avoid exposure to these materials is to handle them only when wearing

proper PPE and using a chemical fume hood. Static charge build-up should be minimized as this can cause increased risk of particle inhalation.

Trialkylphosphine reagents. These reagents, including trioctylphosphine (TOP) and trioctylphosphine oxide (TOPO), are often used during cation exchange reactions and other colloidal syntheses. Proper precautions and thorough review of the SDS for these reagents is critical. They are corrosive to the eyes and skin and are toxic if inhaled. Cation exchange reactions that produce high quality heterostructures require both sonication and heating of trialkylphosphine reagents. These reaction steps have the potential to produce volatile phosphorous containing byproducts that should be assumed as highly toxic through inhalation. Extreme caution should be used when handling TOP and TOP contaminated reaction vessels and equipment, including vials, syringes, and glassware containing residual trioctylphosphine/nanoparticle suspensions and reaction product mixtures. Special care should be taken when cleaning the solvent-trap after synthesis as it can contain condensed, toxic byproducts. TOP is characterized as having a garlic-like odor, which should not be observed if handled correctly.

Reactions under flowing Ar. In general, the methods we use for cation exchange reactions require at least one step that places the reaction vessel under flowing inert gas. There are multiple chemical and physical safety considerations when performing this reaction step. Low boiling point impurities and/or reaction byproducts are evolved as a dense, white vapor that is potentially corrosive and/or toxic. A post-reaction bubbler that contains octadecene or mineral oil is therefore important to help cool and trap the evolved gases. As with all air-free chemical manipulations on a Schlenk line, such processes can, if performed improperly, result in increased pressure inside a closed system, which would constitute an explosion hazard. There must always be an outlet in the Schlenk system (e.g. post-reaction bubbler) to avoid pressure build-up, which may lead to potential explosive shattering of glass Schlenk line components. Again, it is imperative to have proper training and proficiency with air-sensitive manipulations before carrying out such reactions.

Chemical Reagents

Nanoparticle syntheses are well known to be highly sensitive to the quality of the reagents and solvents used, especially the purity and water content.⁴³⁻⁴⁷ Nanoparticle cation exchange reactions are no exception. Below are some highlighted aspects, including physical appearance and the roles of reagents used in the synthesis of roxbyite Cu_{1.8}S template nanoparticles and their transformations using partial cation exchange. All reagents should be handled using appropriate PPE with proper chemical safety training. Personnel should be properly trained and understand the hazards of all reagents *prior to their use*.

Chemical storage. Reagents must be stored according to their specific hazards and recommended storage guidelines. We store all anhydrous metal chloride salts in an airand moisture-free glove box. Each reagent is weighed in the glove box, then removed and immediately transferred to a reaction flask prior to use.

1-Octadecene [ODE, C₁₈H₃₆, technical grade, 90% (Sigma-Aldrich, CAS no. 112-88-9)]. An unsaturated hydrocarbon with a high boiling point (315 °C) that is used as a solvent in many nanoparticle syntheses, including the cation exchange reactions described here. Recent reports have indicated that ODE can polymerize at temperatures that are typical for colloidal reactions,⁴⁸ which can be periodically observed as a coating on nanoparticle products.

Dibenzyl ether [C₁₄H₁₄O, 99% (Acros Organics, CAS no. 103-50-4)]. Dibenzyl ether, which is also referred to as benzyl ether, is used as a common solvent in nanoparticle cation exchange reactions with a high boiling point (298 °C).

Oleylamine [tg-OLAM, C₁₈H₃₇N, technical grade, 70% (Sigma-Aldrich, CAS no. 112-90-3)]. An unsaturated, primary amine that ranges in color from colorless to yellow directly from the chemical supplier. It is used as a surface stabilizing ligand and solvent in the synthesis of Cu_{1.8}S nanorods and cation exchange reactions with a high boiling point (350 °C). This reagent can function as a reducing agent in many nanoparticle syntheses under certain conditions.⁴⁹ The 30% impurity in technical grade OLAM likely consists of other primary and related amines, and some nanoparticle reactions are highly sensitive to these impurities.⁵⁰ Therefore, each reaction described in this work uses tg-OLAM that has been purified through a vacuum distillation process.

Distilled tg-OLAM (d-OLAM). Previous reports call for oleylamine to be distilled over sodium metal or other drying reagents, combined with several other detailed purification steps.⁵⁰ However, we have observed that vacuum distillation alone yields a reagent that consistently produces high-quality nanoparticles and partial cation exchange products compared to the as-received reagent. We typically purify a 500 g bottle of tg-OLAM using a 1000 mL round-bottom flask equipped with a heating mantle, three-way adapter, inlet adapter, alcohol thermometer, condenser, vacuum adapter, receiving flask, and a magnetic stir bar. The distillation product is colorless and leaves behind a yellow to pink liquid in the distillation flask. Details on the process we use for distillation can be found in ref. 24. The purity of our distilled product is not currently known, but the distillation process improves the reproducibility of these reactions. As an alternative, higher purity OLAM (>98%), which offers similar improvements to reproducibility, can be purchased directly, often in small quantities, from some chemical suppliers.

Tri-n-octylphosphine [TOP, $C_{24}H_{51}P$, 85% (TCI America, CAS no. 4731-53-7)]. A viscous, light-yellow to colorless clear liquid that is used as a soft Lewis base to extract soft acids, such as Cu^+ , during cation exchange reactions and as a surface stabilizing ligand in nanoparticle synthesis.

Trioctylphosphine oxide [TOPO, $C_{24}H_{51}OP$, ReagentPlus, 99% (Sigma-Aldrich, CAS no. 78-50-2)]. A flaky, white solid that is typically used as a surface stabilizing ligand and solvent in the synthesis of $Cu_{1.8}S$ nanorods due to its low melting temperature (50 °C) and high boiling point (411 °C).

1-Dodecanethiol [1-DDT, $C_{12}H_{26}S$, \geq 98% (Sigma-Aldrich, CAS no. 112-55-0)]. A common primary alkyl thiol reagent that is a clear, colorless liquid. This reagent is commonly used as a sulfur source and stabilizing ligand in the synthesis of $Cu_{1.8}S$ nanorods.

Tert-Dodecanethiol [t-DDT, C₁₂H₂₆S, mixture of isomers, 98.5% (Sigma-Aldrich, CAS no. 25103-58-6)]. A common tertiary alkyl thiol reagent that is a clear, colorless to slightly yellow liquid. Much like 1-DDT, this reagent is commonly used as a capping ligand and sulfur source in the synthesis of Cu_{1.8}S nanorods.

Copper(II) nitrate trihydrate $[Cu(NO_3)_2 \cdot 3H_2O, 98\% (Sigma-Aldrich, CAS no. 10041-43-3)]$. A blue, hydrated metal salt used as a copper reagent for the synthesis of roxbyite $Cu_{1.8}S$ nanoparticles. It tends to form large clumps that are difficult to break up after long-term storage in air. This aggregation does not affect the reactivity of the reagent.

Zinc(II) chloride [ZnCl₂, anhydrous, >97% (Sigma-Aldrich, CAS no. 7646-85-7)]. A finely divided, deliquescent, white crystalline powder that is used for Zn²⁺ cation exchange reactions. ZnCl₂ will liquify when exposed to air for extended periods of time, so handling this reagent in atmospheric conditions should be minimized.

Cadmium(II) chloride [CdCl₂, anhydrous, 99.99% (Alfa Aesar, CAS no. 10108-64-2)]. A white, hygroscopic crystalline powder used for Cd²⁺ cation exchange reactions as a <u>stoichiometrically limited</u> metal salt reagent. Extreme care should be taken when handling this reagent, as detailed in the previous section.

Cadmium(II) acetate dihydrate [Cd(CH₃COO)₂·2H₂O, reagent grade, 98% (Sigma Aldrich, CAS no. 5743-04-4)]. A white powder, used for Cd²⁺ cation exchange reactions as an <u>excess</u> of metal salt reagent, that is stable for long-term storage in air. As for CdCl₂, extreme care should be taken when handling this reagent, as detailed in the previous section.

Cobalt(II) chloride [CoCl₂, anhydrous, >98% (Sigma-Aldrich, CAS no. 7646-79-9)]. CoCl₂ is a blue, hygroscopic powder used for Co²⁺ cation exchange reactions. It can undergo redox reactions that can lead to a change in oxidation state when dissolved in solution. It likely oxidizes when exposed to air as a solid.

Manganese (II) chloride tetrahydrate [MnCl₂·4H₂O, 98.0-101.0% (Alfa Aesar, CAS no. 13446-34-9)]. A light-pink crystalline solid, used for Mn²⁺ cation exchange reactions, that can be stored in air. This salt can sometimes contain brown flakes, which are insoluble in the reaction medium. If such insoluble impurities are present, consider purchasing a new reagent. We have found that many as-received anhydrous MnCl₂ reagents contain this impurity, therefore we prefer to use the hydrated form instead.

Indium(III) chloride [InCl₃, anhydrous, 98% (Alfa Aesar, CAS no. 10025-82-8)]. InCl₃ is a white, flaky solid, used for In³⁺ cation exchange reactions, that is moisture sensitive.

Synthesis and Characterization of Roxbyite Copper Sulfide Nanorods

Copper sulfide is a widely used template for nanocrystal cation exchange because it can be synthesized as nanoparticles that adopt a variety of sizes, shapes, and crystal structures. Our focus here is on partial cation exchange using roxbyite Cu_{1.8}S nanorods (20 x 50 nm, aspect ratio 2.5), although the length (and therefore aspect ratio) can be tuned if desired. Nanorods can be synthesized in >100 mg batches and through cation exchange, can be transformed into tens of thousands of possible partial cation exchange products. The reaction that we use, which produces >100 mg of roxbyite Cu_{1.8}S nanorods, is from a published procedure. A detailed description of the synthetic protocol, along with common mistakes and troubleshooting tips, is included below, and a schematic is shown in Figure 3.

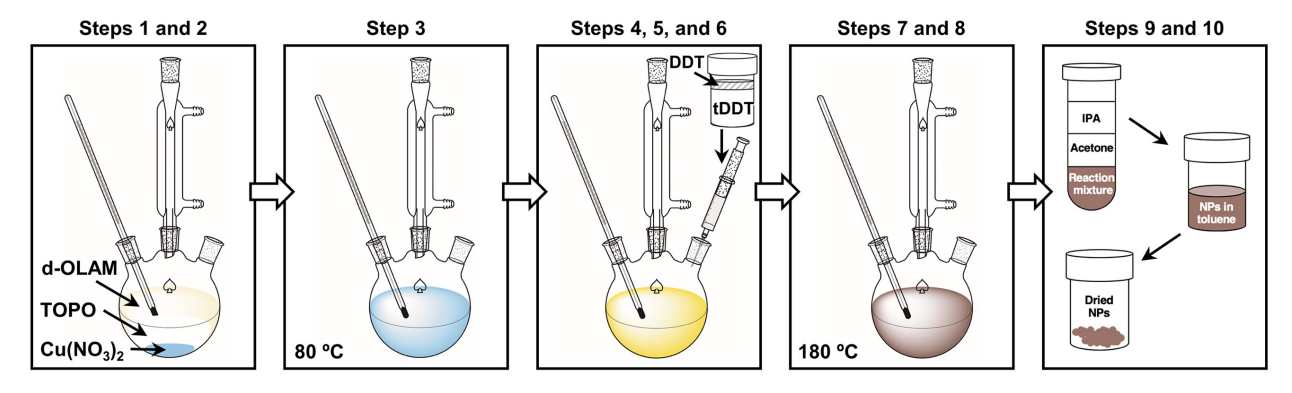


Figure 3. Visual representation of reaction steps involved in the synthesis of roxbyite Cu_{1.8}S nanorods. The step numbers correspond to the reaction steps outlined below. The colors of the solutions and the reaction products are representative of the expected colors for each step.

- (1) Reaction setup. (Figure S1) shows a generic reaction setup. For this synthesis, use a 250-mL three-neck round bottom flask with 14/20 ground glass adapters. The reaction requires a rapid heat-up step, which requires a larger reaction vessel than may be expected, given the relatively small reaction volume of ~35 mL. In general, a reaction flask that has a volume that is ~7 times larger than the reaction volume is desired for this reaction; this requirement should be kept in mind if attempting to scale the reaction up or down.
- (2) Addition of reagents to the flask. Combine 844 mg of Cu(NO₃)₂·3H₂O, 8.7 g of TOPO, and 750 μL of d-OLAM in the 250-mL three-neck round bottom flask, then add a condensing column, thermometer adapter, alcohol thermometer, and stir bar. Attach the reaction flask to a Schlenk line. We highly recommend using the gas-flow adapter with stopcock (Figure S1H) to provide an easy and safe means to place the reaction under flowing inert gas, described in the next step.

- (3) Place reaction flask under vacuum to degas. While at room temperature, slowly place the reaction flask under vacuum, then heat the reaction vessel to 80 °C while stirring and maintain this temperature for 30 minutes. During this time, the solid TOPO and the Cu(NO₃)₂·3H₂O will dissolve and form a clear, light-blue solution. It is important not to exceed 90 °C during the degas step. Heating beyond this temperature results in a color change from blue to green, which could result from reduction of Cu²⁺ to Cu⁺. This causes the reaction product to be inconsistent in size and shape based on empirical observation.
- (4) Tasks while the reaction flask is degassing. While the reaction flask is degassing under vacuum, two additional tasks can be performed. First, prepare 22 mL of a 10:1 v/v solution of tert-dodecanethiol:1-dodecanethiol in a septum capped vial. Using a needle line attached to the Schlenk line, place the vial containing this mixture under vacuum for at least 20 minutes before placing the contents under a blanket of Ar. Second, during the final 10 minutes of the degas step, preheat a second heating mantle. Our standard method for doing this is to attach another heating mantle to a second Variac and set the voltage output to ~80%, although this will be different for different setups and heating systems. Note that this pre-heated mantle can get extremely hot, and therefore it should be handled carefully.
- (5) Cycle with Ar and vacuum. After 30 minutes under vacuum at 80 °C, cycle the reaction vessel with vacuum and Ar twice, then place the reaction flask under a blanket of Ar.
- (6) Addition of t-DDT:DDT. Prepare a 30-mL syringe for injection into an air-free environment and draw 22 mL of the t-DDT:1-DDT mixture into the syringe, then place the reaction vessel, now under a blanket of Ar and still at 80 °C, into the preheated heating mantle. Rapidly inject the t-DDT:1-DDT mixture into the reaction flask at 80°C and place the flask under flowing Ar. The reaction temperature should only drop a few degrees (if at all) after injection before beginning to rapidly increase.
- (7) Heating the reaction. Rapidly heat the flask to 180 °C by wrapping it in aluminum foil or glass wool while it is in the preheated mantle. Ideally, the heat-up from 80 °C to 180 °C should be completed in less than 5 minutes. While heating, the color of the solution should change from blue to yellow, and a dark-green liquid along with white vapor should be expelled from the reaction mixture. In some reactions, we have observed an intermediate change to a cloudy white mixture prior to the reaction color changing to clear yellow. We attribute this is the formation of a copper-thiolate complex at low temperature,⁵³ which does not change the reaction outcome. Note that care should be taken to not exceed 190 °C during any stage of the reaction. Failing to heat the reaction vessel rapidly and/or exceeding 190 °C can cause loss of morphological yield and variability of nanorod aspect ratio based on empirical observation.
- (8) Reaction progress and cooling. Upon reaching 180 °C, the color of the solution should gradually change from yellow to light brown over ~1 minute; it will continue to darken and form a turbid brown suspension over the next several minutes. After maintaining a reaction temperature of 180 °C for 15 minutes, cool the reaction to

room temperature by submerging the reaction flask in a room temperature water bath. Split the contents of the reaction flask between an appropriate number of centrifuge tubes for subsequent cation exchange reactions. As a reminder, the thiol mixture has a strong odor. Product isolation steps that require opening reaction flasks or centrifuge tubes should be performed in a chemical fume hood and a bleach solution should be used to quench these reagents during glassware and centrifuge tube cleaning.

- (9) Isolation and purification. Purify the reaction product via centrifugation using toluene as a solvent and a mixture of isopropanol and acetone as an antisolvent. Throughout this washing procedure, we do not add surfactant to the nanoparticle suspension to make the drying process easier. Disperse the particles in ~15 mL of toluene and transfer them to a septum capped vial. Allow the particles to settle from the suspension, typically overnight, and then decant off the clear supernatant. Evaporate the remaining toluene by drying the suspension under vacuum. After the particles are dry, the vial can be opened to atmosphere. Scrape the nanoparticle film into a powder and gently grind the powder to break up large aggregates using a plastic spatula. As a reminder, dry powders of nanoparticles should be treated as hazardous and therefore should only be handled after evaluating safety procedures and using proper PPE.
- (10) Storage. For purposes of achieving consistent masses, we choose to dry the roxbyite Cu_{1.8}S into a powder and store them in a septum capped vial, but they can be stored in suspension without impacting their cation exchange behavior. These particles are stable for several weeks without a noticeable change in their morphology or partial cation exchange behavior, though we have not conducted an exhaustive study on their longer-term stability or reactivity.

Key characterization data for roxbyite Cu_{1.8}S nanorods includes TEM images, statistical analysis of particle size, and XRD patterns, as shown in Figure 4. The nanorods tend to orient horizontally on the TEM grid, although occasionally they can bundle so that the nanorods align vertically. Several compositionally related copper sulfide phases have large and low-symmetry unit cells, and it can be difficult to differentiate them, especially in nanoparticles having small and/or poorly crystalline domains. Figure 4C shows an experimental diffraction pattern of roxbyite Cu_{1.8}S nanorods compared to simulated diffraction patterns for three structurally similar phases of copper sulfide: roxbyite, djurleite, and monoclinic chalcocite. Roxbyite Cu_{1.8}S can be identified by characteristic reflections at 26.5°, 29.7°, and 31.2° 2θ, which have the greatest intensity and diffraction angle differences between other common phases.

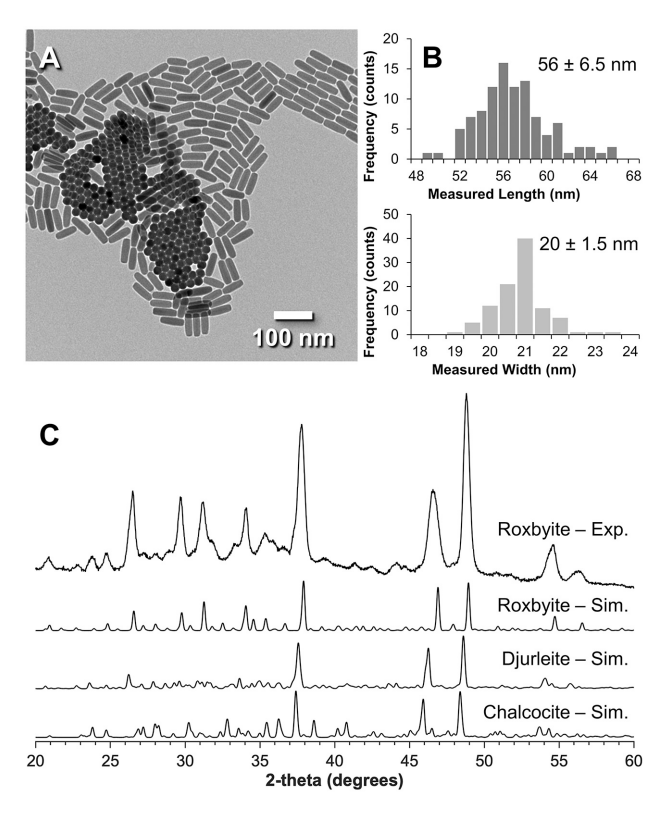


Figure 4. Key characterization data for roxbyite Cu_{1.8}S nanorods. (A) A bright-field TEM image of roxbyite Cu_{1.8}S nanorods shows their anisotropic morphology and their tendency both to lay horizontally and to form hexagonally packed bundles that lay vertically. (B) Histograms show the size-distribution of their lengths (top) and widths (bottom). (C) A powder XRD pattern of roxbyite Cu_{1.8}S nanorods is compared to simulated reference patterns for roxbyite (Cu_{1.8}S), djurleite (Cu_{1.94}S), and monoclinic chalcocite (Cu₂S). The best match is to roxbyite Cu_{1.8}S, with differences in peak shape and intensities attributed to preferred orientation due to the nanorod morphology. Panels (B) and (C) were adapted with permission from ref. 24. Copyright 2020 American Association for the Advancement of Science.

Preferred orientation is commonly observed for the roxbyite Cu_{1.8}S nanorods due to the anisotropic crystallite shape. This results in enhancement of the reflections at 34.1°, 37.9°, and 48.9° 2θ due to preferential alignment of the nanorods along their long axes, which are in the crystallographic *a*-direction of roxbyite Cu_{1.8}S. Note that preferred orientation causes concomitant suppression of many other planes that orient perpendicular to the diffraction plane, such as (064), which appears at 46.9° 2θ. Djurleite, a structurally related phase of copper sulfide that is slightly more copper-rich than roxbyite, sometimes appears as an impurity in samples of the Cu_{1.8}S nanorods. Morphologically, the djurleite nanorods are identical to the roxbyite nanorods, and their cation exchange behavior is similar as well. It is worth noting that djurleite typically transforms to roxbyite over a period of several weeks of storage under ambient conditions, so the nanorods will essentially "self-purify" to roxbyite.

Preparation of Cation Exchange Solutions

Many metal salts are commercially available and have been used for cation exchange reactions. Certain counterions can impact cation exchange reactions.⁵⁴ although further work is required to fully understand their roles. We have encountered similar counterion effects, especially when attempting sequential partial cation exchange reactions in which multiple counterions are present. Therefore, when possible, we maintain consistency in counterions and prefer to use anhydrous metal chlorides whenever possible. The anhydrous metal salts are stored in a dry glovebox with an argon atmosphere. Each metal salt is used immediately after removing the appropriate mass from the glove box, thereby limiting its exposure to air and water. For cation exchange reactions for which metal chloride salts cannot be used due to solubility issues, we use hydrated metal acetates. All cation exchange solutions are prepared using published procedures, 23,24 and can be used for both partial cation exchange reactions using excess metal salt reagents and partial cation exchange reactions using stoichiometrically limited metal salt reagents, depending on conditions used in the cation exchange process. The method used to prepare cation exchange solutions is outlined below. A schematic of these steps is shown in gray in Figure 5.

- (1) Reaction setup and addition of reagents. In a 50-mL three-neck round bottom flask, add the appropriate mass of the desired metal salt, as shown in Table S2, then add 15 mL of benzyl ether, 8 mL of distilled oleylamine (d-OLAM), and 2 mL of octadecene. Equip the flask with a condensing column, thermometer adapter, alcohol thermometer, and stir bar and attach it to a Schlenk line, as described in the preceding section on roxbyite Cu_{1.8}S nanoparticle synthesis.
- (2) Place the reaction under vacuum to degas. Begin stirring the metal salt mixture and place the reaction flask under vacuum slowly to prevent vigorous bumping. Leave the flask under vacuum and heat the reaction solution to 120 °C for 30 minutes. During this step, the metal salt should begin to dissolve. Some metal salts, including InCl₃ and MnCl₂, have a high propensity to decompose to form oxides upon heating. For these, hold under vacuum for 60 minutes, instead of 30 minutes for the others. For Cd(acetate)₂, the cation exchange solution is fully prepared at this point; additional heating is not required. For all other salts, steps 3 and 4 are required.

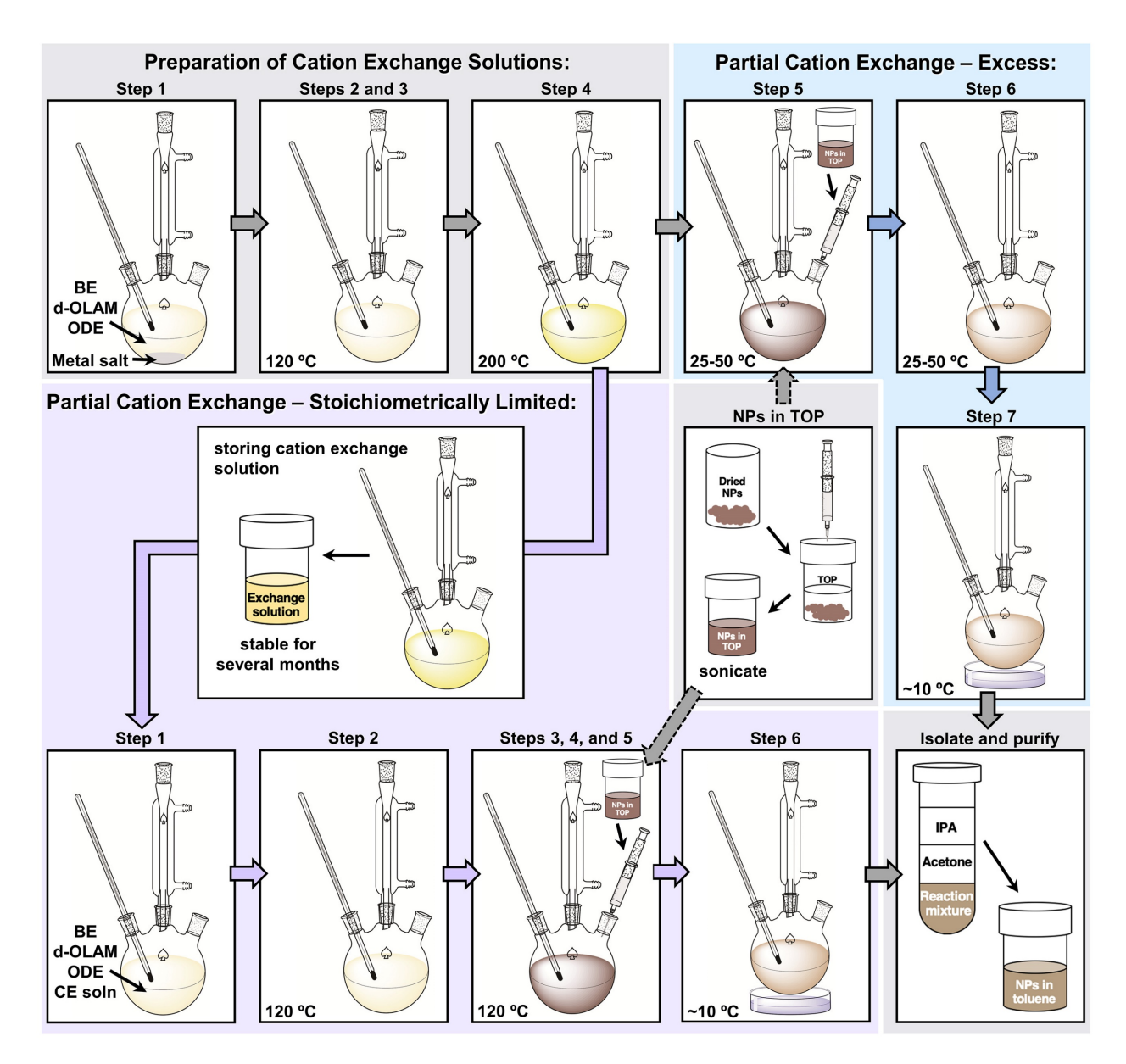


Figure 5. Visual representation of the reaction steps involved in partial cation exchange reactions. Reaction steps that are the same for both reaction pathways (preparation of cation exchange solutions, formation of TOP/Cu_{1.8}S suspension, and isolation of particles through centrifugation) are shown in gray. Steps unique to partial cation exchange using excess reagents are shown in blue, and those that are unique to partial cation exchange using stoichiometrically limited reagents are shown in purple. Each step in the sequence matches the steps shown in the respective experimental procedures in the next sections. The colors of the solutions and the reaction products are representative of the expected colors at each step for exchange with Zn^{2+} .

- (3) Cycle with Ar and vacuum. Place the reaction flask under a blanket of Ar, then cycle three times with Ar and vacuum. After cycling, place the reaction under flowing Ar.
- (4) Heating the reaction and reaction progress. Increase the reaction temperature to 200 °C and maintain this temperature for 30 minutes. During this time, the reaction

- mixture should form a clear solution with colors matching those shown in Figure 6B. If the color of the solution is different than expected, consult the troubleshooting section below.
- (5) Cooling and use in cation exchange pathway. At this point, the solution can be cooled to a desired reaction temperature and used directly for partial cation exchange reactions using <u>excess</u> metal salt reagents. For partial cation exchange reactions using <u>stoichiometrically limited</u> metal salt reagents, the exchange solution can be stored after being transferred to a septum capped vial using a syringe (if using ZnCl₂, CdCl₂, Cd(acetate)₂, or InCl₃) or be kept in the reaction flask for later removal of a portion to use directly (if using CoCl₂ or MnCl₂). Consult the troubleshooting section for additional insights.

Troubleshooting: Cation Exchange Solution Preparation and Storage

Cation exchange solutions are prepared using nearly identical conditions and the same combinations of ligands and solvents. Effective preparation and, in some cases, storage of these solutions is critical to the success of cation exchange reactions.

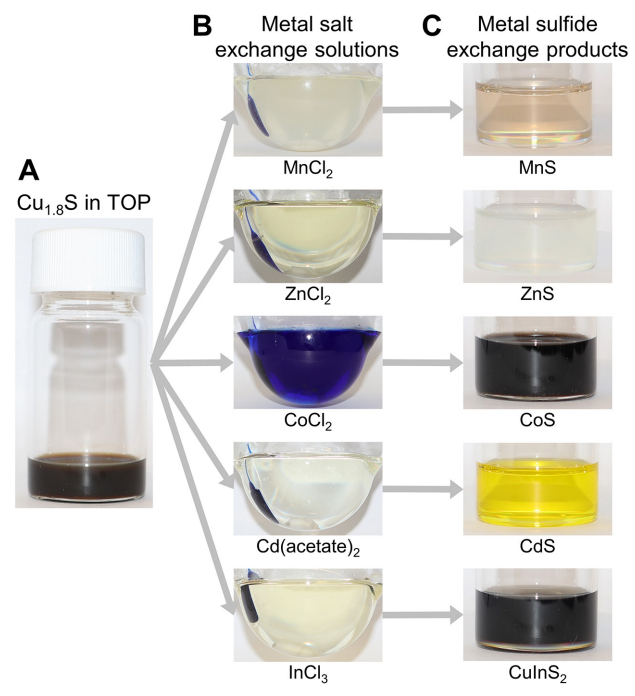


Figure 6. Photographs of the solutions containing the reactants and the products of complete cation exchange. (A) Suspension of roxbyite Cu_{1.8}S nanorods in TOP after sonicating for 45 minutes. (B) Cation exchange solutions prepared using (from top to bottom) MnCl₂, ZnCl₂, CoCl₂, Cd(acetate)₂, and InCl₃. Note the color and clarity of the solutions. (C) Suspensions of the products obtained by complete exchange of the Cu⁺ cations in roxbyite Cu_{1.8}S with the cations from the exchange solutions in (B). The products are (from top to bottom) MnS, ZnS, CoS, CdS, and CuInS₂.

Preparation. It is important to monitor the color of exchange solutions during their preparation, as the color provides useful insights into purity and oxidation state. Exchange

solutions prepared from MnCl₂ (yellow), CoCl₂ (blue), ZnCl₂ (yellow), Cd(acetate)₂ (colorless), and InCl₃ (colorless) are shown in Figure 6B. All of the exchange solutions are clear. We have found that metal salt purity and age are the main contributors to inconsistencies in the cation exchange solutions and the resulting cation exchange behavior. We use metal salts that have a purity greater than 97% with colors matching those described by the supplier. In most cases, we limit long-term storage under atmospheric conditions to avoid degradation, hydration, and oxidation. Visible impurities, such as flakes or clumps that do not match the expected reagent color, are obvious when present, such as those shown for MnCl₂ in Figure S2. These impurities may result in exchange solutions and reaction products that do not match the expected color or quality. Other "impurities" such as water content for hygroscopic or deliquescent salts, must also be considered. Water content that is unknown or not accounted for in a hydrated metal salt can impact stoichiometry and concentration due to mass differences that are not considered during weighing.

Storage. Only small quantities of cation exchange solution are needed for partial cation exchange reactions using stoichiometrically limited metal salt reagents. Storing a stock solution can be convenient, but it is important to know which solutions can be stored and which cannot. Cation exchange solutions prepared using ZnCl₂, InCl₃, or Cd(acetate)₂ remain clear at room temperature. They can be transferred to clean septum-capped vials directly from the reaction flask via syringe for storage over a period of several months without degradation or change in reactivity. Exchange solutions prepared using CdCl₂ form a white precipitate upon cooling that can dissolve or melt at moderate temperatures (50-60 °C). This exchange solution should be transferred to a septum-capped vial while warm and must be heated prior to use. Cation exchange solutions prepared from MnCl₂ quickly and irreversibly change color from yellow to dark brown over a period of several minutes, and a pale brown precipitate begins to form after several hours. This occurs even in a tightly fitting septum capped vial that is stored under Ar. Exchange solutions prepared from CoCl₂ also undergo a rapid color change, from dark blue to dark red (Figure S3). This process can be reversed upon heating to ~120 °C for more than 30 minutes. However, we have experienced reactivity issues if these criteria are not met precisely. For these reasons, we use Mn²⁺ exchange solutions prepared from MnCl₂ and Co²⁺ exchange solutions prepared from CoCl₂ immediately after preparation instead of storing them.

Partial Cation Exchange Reactions Using Excess Metal Salt Reagents

One way to carry out partial cation exchange reactions is to use a significant excess of metal cations relative to the number of Cu⁺ cations in the roxbyite Cu_{1.8}S template, and then use reaction time or temperature to control the extent of partial exchange. For example, partial cation exchange on roxbyite Cu_{1.8}S nanorods using an <u>excess</u> of Zn²⁺ occurs over 90 minutes at 50 °C. Figure 7 shows TEM images and STEM-EDS element maps of aliquots taken during the 90-minute reaction. These aliquots reveal the precise degree of control that can be achieved by temporally modulating the extent of exchange in partial cation exchange reactions using <u>excess</u> metal salt reagents. The procedure below is reproduced from a published protocol²³ and is representative of the exchange

performed on roxbyite Cu_{1.8}S nanorods to produce the ZnS–Cu_{1.8}S heterostructures in Figure 7. A schematic for this reaction is shown in blue in Figure 5. A similar procedure can be performed using other roxbyite Cu_{1.8}S nanoparticle shapes or with other exchanging cations using the metal salts and reagent quantities shown in Table S2.

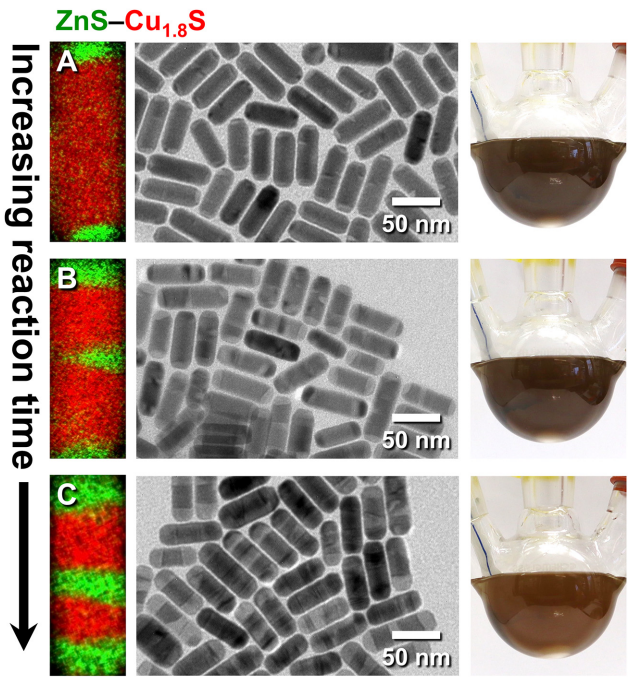


Figure 7. Time-dependence of a partial cation exchange of roxbyite $Cu_{1.8}S$ nanorods using excess Zn^{2+} . The figure shows STEM-EDS element maps (left), bright-field TEM images (center), and photographs of the corresponding reaction flasks (right) at reaction times of (A) 15 minutes, (B) 30 minutes, and (C) 90 minutes. As the reaction progresses, more ZnS is incorporated into the $Cu_{1.8}S$ nanorods and the color of the nanorod suspension becomes a lighter brown. In the STEM-EDS element maps, the Zn Kα and Cu Kα lines are shown in green and red, respectively. The dark regions in the TEM images of the nanorods are $Cu_{1.8}S$ and the brighter regions are ZnS. The STEM-EDS element maps and bright-field TEM images were adapted with permission from ref. 23. Copyright 2018 American Association for the Advancement of Science.

- (1) Cooling prepared exchange solution to desired reaction temperature. Follow the procedure outlined in the Preparation of Cation Exchange Solutions section, then decrease the temperature of the reaction flask to the reaction temperature required to achieve the desired level of partial cation exchange. For typical cation exchange reactions using excess metal salt reagents, we use a temperature range between room temperature and 50 °C, with the specific temperature chosen through empirical optimization. For the Zn²⁺ exchange shown in Figure 7, a Zn²⁺ exchange solution was prepared using the procedure detailed in the previous section and then maintained a reaction temperature of 50 °C.
- (2) Addition of TOP to Cu_{1.8}S nanorods. Weigh out 12 mg of Cu_{1.8}S nanorods in dried powder form into a clean septum-capped vial. Place this vial under vacuum using a needle line attached to a Schlenk line, then place the vial under a blanket of Ar.

Prepare a syringe for injection, then withdraw 3 mL of TOP and inject it into the vial containing the $Cu_{1.8}S$ nanorods. Immediately place the vial under vacuum, then cycle with Ar and vacuum before placing the vial under a blanket of Ar. The temperature of the flask should not drop substantially upon addition of this suspension. A decrease of ~5 °C is normal, but the temperature should recover and stabilize at 50 °C within a few minutes for best results. Complete details on the effect of temperature on this reaction can be found in the Troubleshooting section.

- (3) Sonicate to form TOP/Cu_{1.8}S suspension. Sonicate the TOP/Cu_{1.8}S suspension at room temperature for 45 minutes. This step is important for obtaining consistent partial cation exchange products. Safety considerations are paramount for this step, so it is important to review the Safety Considerations section and SDS for trioctylphosphine. Proper use of a well-functioning chemical fume hood is critical to ensure that there is no exposure to volatile phosphine-containing byproducts.
- (4) *Inject the TOP/Cu_{1.8}S suspension.* Ensure that the temperature of the reaction flask is stable, then swiftly inject the brown TOP/Cu_{1.8}S nanoparticle suspension into the flask. Immediately place the reaction flask under vacuum, then cycle with Ar and vacuum before placing the flask under a blanket of Ar.
- (5) Reaction progress and aliquot removal. Allow the reaction to proceed for the desired amount of time, which is defined by the reaction temperature and the exchange rate of the cations. When performing a cation exchange reaction for the first time, we remove and analyze aliquots (typically at 5, 15, 30, 60, and 120 minutes) to empirically determine the extent of partial cation exchange over time. To remove an aliquot, first prepare a syringe for injection into the reaction flask, then withdraw a small portion (0.2 0.5 mL) and inject the aliquot into a centrifuge tube containing antisolvent; the centrifuge tube containing antisolvent should be in an ice bath to help quench the cation exchange reaction. Immediately cycle with vacuum and Ar while simultaneously isolating the product via centrifugation.
- (6) Cooling in an ice bath. When the reaction is complete and/or the desired number of aliquots have been removed, place the entire reaction vessel in an ice bath to rapidly cool it to ~10 °C. Cooling the reaction in an ice bath arrests the partial cation exchange at the desired time and reduces the chance of undesired dissolution of residual Cu_{1.8}S upon exposure to atmosphere.
- (7) Isolation, purification, and storage. Once the temperature is ~10 °C, remove the septum from the reaction flask and transfer the contents into an appropriate number of centrifuge tubes. Purify the product via centrifugation using toluene as a solvent and a 1:1 v/v mixture of isopropanol and acetone as an antisolvent. Resuspend the product in ~ 5mL of toluene. We typically do not add surfactant to our storage suspensions because the particles suspend well in toluene and oleylamine may cause slight dissolution of the Cu_{1.8}S regions. ⁵⁶ This product can be stored for several days before characterization or use in other reactions.

The aliquots that are removed during the partial cation exchange reactions can be analyzed using TEM and XRD, as discussed in the Characterization of Heterostructured Nanoparticles section. They can also be analyzed optically or visually, because in many

cases, the colors of the cation exchange product are different than the color of the roxbyite $Cu_{1.8}S$ template nanoparticles (Figure 6). Figure 7 shows the evolution of color over the course of a partial cation exchange reaction that uses an excess of exchanging Zn^{2+} cations to produce a wurtzite ZnS product.

Partial cation exchange reactions using <u>excess</u> metal salt reagents, in which the extent of exchange controlled by time and/or temperature, typically produce heterostructured nanoparticles that contain multiple exchanged regions. The formation of multiple exchanged regions in each nanoparticle results from the initiation of cation exchange at multiple sites within the template nanoparticle at early stages of the reaction, due to the significant excess of exchanging cations; these regions then grow larger as the reaction progresses. For cation exchange products that require large volume expansions relative to the roxbyite Cu_{1.8}S template, i.e. CdS which requires a volume expansion of 14% relative to Cu_{1.8}S, a smaller number of exchanged regions form in the heterostructured nanoparticle product. If the size of the template roxbyite Cu_{1.8}S nanoparticle is large enough, however, multiple exchange regions are still observed.²³ All of these factors must be considered when designing a partial cation exchange reaction to produce a targeted heterostructured nanoparticle.

Partial Cation Exchange Reactions using Stoichiometrically Limited Metal Salt Reagents

It is also possible to achieve partial cation exchange by designing it to be self-limiting using only a sub-stoichiometric quantity of exchangeable cations. Partial cation exchange reactions using <u>stoichiometrically limited</u> reagents have been used effectively in several cases to produce complex heterostructured products. Stoichiometrically limited partial cation exchange occurs by adding specific volumes of exchange solutions that have known concentrations. This method enables semi-quantitative control over the extent of cation exchange, and the amounts can be calculated using simple stoichiometric relationships, as shown in Equation 1:

Volume_{exchange solution} = Fraction of exchange
$$\times \left[\frac{\text{moles of copper sulfide used}}{\text{oxidation state}_{\text{exchanging cation}} \times \text{concentration}_{\text{exchange solution}} \right]$$
 (1)

For example, the volume of exchange solution required in a reaction that targets a 50% fraction of exchange using 18 mg of Cu_{1.8}S nanorods (MW: 145.18 g/mol) and the Zn²⁺ exchange solution prepared using the mass from Table S2 can be estimated as:

Volume_{exchange solution}=
$$0.50 \times \left[\frac{0.124 \text{ mmol}}{2 \times 0.073 \text{ mmol/mL}}\right] = 0.425 \text{ mL}$$

Figure 8 contains HAADF-STEM images and STEM-EDS element maps highlighting the tunability in cation exchange that can be achieved using this reaction pathway, simply by varying the amount of the exchange solution that is added. Empirically, we observe close agreement between the intended fraction of exchange calculated using Equation 1 and the actual experimentally observed extent of exchange in our heterostructured products. However, the agreement is not quantitative, and should only be considered as an

approximation for several reasons. First, the number of moles of Cu_{1.8}S used in Equation 1 is only an approximate. We determine the mass of template roxbyite Cu_{1.8}S nanorods gravimetrically and assume, for simplicity, that this mass corresponds to *only* copper sulfide with a stoichiometry of Cu_{1.8}S and a molecular weight of 145.15 g/mol. This is a reasonable approximation, but it is important to remember that the measured mass includes the mass of the particles and the mass of the ligands that stabilize their surfaces. Instead of estimating ligand coverage, which requires additional assumptions, we choose to overestimate the true mass of the copper sulfide present by assuming that the total mass corresponds to the Cu_{1.8}S nanorods. Second, the concentration determined for each exchange solution assumes quantitative transfer and utilization. Several hundred microliters to one milliliter of the solvent mixture are lost during the Ar flow step. Therefore, the exchange solution concentration is slightly underestimated relative to the true concentration. Despite these assumptions and approximations, Equation 1 is very reliable and useful for dialing in a desired extent of partial cation exchange using stoichiometrically limited reagents.

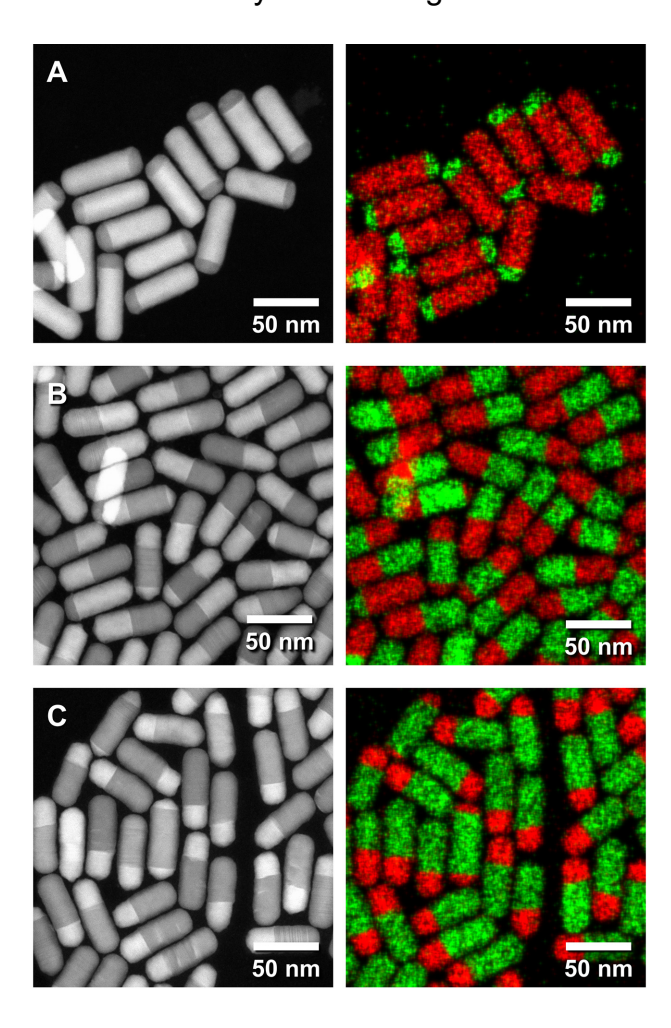


Figure 8. Tunable extent of exchange during partial cation exchange of roxbyite $Cu_{1.8}S$ nanorods using stoichiometrically limited quantities of Zn^{2+} . HAADF-STEM images (left) and STEM-EDS element maps (right) are shown for three samples prepared using different quantities of 0.073 mol/mL Zn^{2+} exchange solution. Single-tip $ZnS-Cu_{1.8}S$ nanorods, with different relative lengths of the ZnS and $Cu_{1.8}S$ segments, were prepared by (A) targeting a 25% extent of exchange and using 212 μ L of Zn^{2+} exchange solution, (B)

targeting a 50% extent of exchange and using 425 μ L of Zn²⁺ exchange solution, and (C) targeting a 75% extent of exchange and using 850 μ L of Zn²⁺ exchange solution. In the STEM-EDS element maps, the Zn K α and Cu K α lines are shown in green and red, respectively. In the HAADF-STEM nanorod images, the darker regions are ZnS and the brighter regions are Cu_{1.8}S.

We have applied the concept of partial cation exchange reactions using <u>stoichiometrically</u> <u>limited</u> reagents to propose synthetically feasible reaction pathways to 65,520 distinct heterostructured nanorods, highlighting how this process can be used as a design principle to produce a megalibary containing any combinations of ZnS, CdS, CoS, Cu_{1.8}S, CuInS₂, and CuGaS₂ segments.²⁴ Heterostructured nanoparticles produced using <u>stoichiometrically limited</u> reagents generally have fewer exchange regions than partial cation exchange reactions produced using <u>excess</u> reagents with the same cation(s). It is important to consider this behavior when targeting specific heterostructured products. As a representative example, the procedure to produce roxbyite Cu_{1.8}S nanorods having a single ZnS tip, in high yield (>87%), is reproduced from ref. 24 below. A schematic of this reaction is shown in purple in Figure 5.

- (1) Addition of reagents and cation exchange solution. Add 7.5 mL of benzyl ether, 4 mL of d-OLAM, 1 mL of ODE, and the desired quantity of any cation exchange solution prepared above. As an example, the volume of exchange solution for the samples shown in Figure 8 were determined from calculating the needed quantity for 25%, 50%, and 75% extent of exchange. These volumes were 212 μL, 425 μL, and 850 μL, respectively. Equip the flask with a condensing column, thermometer adapter, alcohol thermometer, rubber septum, and stir bar and attach it to a Schlenk line.
- (2) Place the reaction under vacuum to degas. Begin stirring the solution while at room temperature. Place the reaction vessel under vacuum slowly and heat the contents to 120 °C while stirring for 30 minutes. Place the flask under a blanket of Ar, then cycle with Ar and vacuum and place the reaction vessel under a blanket of Ar.
- (3) Addition of TOP to Cu_{1.8}S nanorods. During the degas step, weigh out 18 mg of Cu_{1.8}S nanorods in dried powder form into a clean septum-capped vial. Place this vial under vacuum using a needle line attached to a Schlenk line, then cycle the atmosphere of the vial with Ar and vacuum before placing the vial under a blanket of Ar. Prepare a syringe for injection, then withdraw 1.5 mL of TOP and inject it into the vial containing the Cu_{1.8}S nanorods. Immediately place the vial under vacuum, then cycle with Ar and vacuum before placing the vial under a blanket of Ar.
- (4) Sonicate to form TOP/Cu_{1.8}S suspension. Sonicate the TOP/Cu_{1.8}S suspension at room temperature for 45 minutes. This step is important for obtaining consistent partial cation exchange products. Safety considerations are paramount for this step, so it is important to review the Safety Considerations section and the SDS for trioctylphosphine. Proper use of a well-functioning chemical fume hood is critical to ensure that there is no exposure to volatile phosphine-containing byproducts.
- (5) *Inject the TOP/Cu_{1.8}S suspension and reaction progress.* Inject the contents of the TOP/nanoparticle suspension into the reaction flask at the desired reaction temperature for each cation, as shown in Table S3. Then, provided that the reaction

temperature is below 130 °C, cycle with Ar and vacuum. The temperature of the reaction flask may drop by ~10 °C but should recover within 3-5 minutes. Complete details on the effect of temperature on this reaction can be found in the Troubleshooting section. We have most extensively studied the behavior of stoichiometrically limited exchange with Zn²+. Through empirical optimization, we found that injecting the TOP/nanoparticle suspension at a temperature of 120 °C or higher produces the highest percentage of single-tip ZnS–Cu_{1.8}S nanorods. For <u>stoichiometrically limited</u> Zn²+ exchanges, injecting the TOP/Cu_{1.8}S suspension at temperatures lower than 120 °C results in different exchange patterns or a mixture of products. Consult the Troubleshooting section for details. For a Zn²+ exchange to produce single-tip ZnS–Cu_{1.8}S nanorods, allow the reaction to proceed for 30 minutes at 120 °C

- (6) Cooling in an ice bath., After maintaining the reaction for the time in Table S3, place the entire reaction vessel in an ice bath to rapidly cool it to ~10 °C. Cooling the reaction in an ice bath reduces the chance of undesired dissolution of residual Cu_{1.8}S upon exposure to atmosphere.
- (7) Isolation, purification, and storage. Once it is at ~10 °C, remove the septum from the reaction flask and transfer the contents into an appropriate number of centrifuge tubes. Purify the product *via* centrifugation using toluene as a solvent and a 1:1 v/v mixture of isopropanol and acetone as an antisolvent. Resuspend the product in ~5 mL of toluene. We typically do not add surfactant to our storage suspensions because the particles suspend well in toluene and oleylamine may cause slight dissolution of the Cu_{1.8}S regions.⁵⁶ This product can be stored for several days before characterization or use in other reactions.

The procedure above outlines a stoichiometrically limited partial cation exchange reaction to produce the single-tip ZnS–Cu_{1.8}S nanorods shown in Figure 8. This approach can be used for additional exchanges with other cations instead of Zn²⁺, such as Co²⁺, Cd²⁺, In³⁺, and Ga³⁺, and does *not* require the products to be isolated between reaction steps.²⁴ The process for sequential partial cation exchange is very similar to that outlined above for the first step: desired quantities of cation exchange solutions are calculated using Equation 1 and injected into the reaction flask at specific temperatures and allowed to react to completion in sequence. This process can then be repeated as desired until there is either no more Cu⁺ left to react or the desired number of steps have been completed. Figure 9 shows a few examples used to create tens of milligrams of heterostructured products obtained through multiple partial exchange steps.²⁴

Troubleshooting

This troubleshooting section describes synthetic challenges that can lead to the formation of undesired products, sample degradation, batch-to-batch variation, and other factors that can negatively impact partial cation exchange reactions. Partial exchange with Zn^{2+} on $Cu_{1.8}S$ nanorods is used as a model system, and any modifications described in this section are relative to the "standard" partial cation exchange conditions corresponding to each of the two pathways – excess reagents or stoichiometrically limited reagents –

detailed above. Troubleshooting guides should be considered as suggestions, as some are based on ongoing research and/or preliminary observations. Table S4 provides some of the most common troubleshooting issues that are encountered in partial cation exchange reactions.

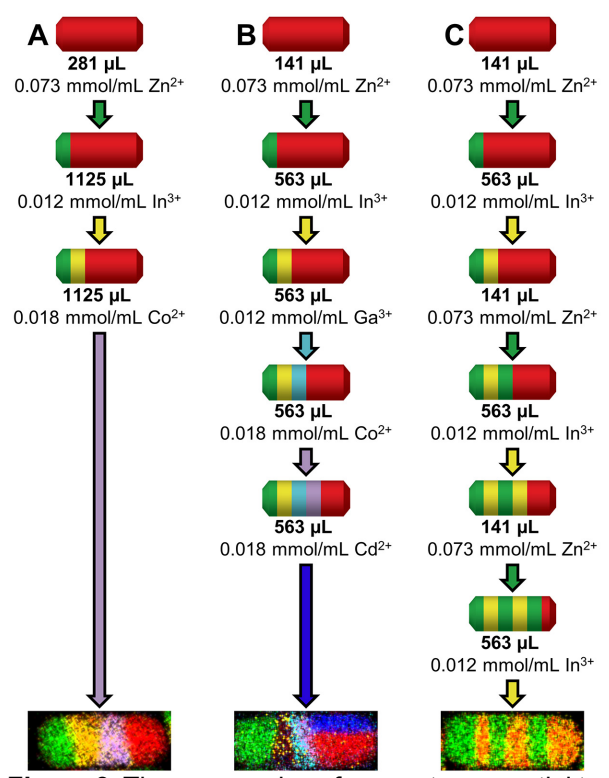


Figure 9. Three examples of one-pot, sequential transformations of roxbyite $Cu_{1.8}S$ nanorods using multiple partial cation exchange steps and stoichiometrically limited metal salt reagents. (A) $ZnS-CulnS_2-CoS-Cu_{1.8}S$ can be synthesized by sequentially injecting exchange solutions of Zn^{2+} , In^{3+} , and Co^{2+} . (B) $ZnS-CulnS_2-CuGaS_2-CoS-(CdS-Cu_{1.8}S)$ can be synthesized by sequentially injecting exchange solutions of Zn^{2+} , In^{3+} , Ga^{3+} , $Ga^{$

Mass of Cu_{1.8}S nanoparticles. A significant source of variability in both cation exchange pathways is caused by variations in the quantity of template roxbyite Cu_{1.8}S nanoparticles used in the reactions. The preceding section discussed assumptions made in calculating the mass of roxbyite Cu_{1.8}S nanoparticles, which makes it approximate. Consistency in mass determination is the most important factor in maximizing reproducibility. We prefer to determine the mass of a dry nanoparticle powder generated immediately after their synthesis, i.e. the roxbyite Cu_{1.8}S nanoparticles are collected by centrifugation and dried to a powder immediately rather than being stored as a colloidal suspension. Drying nanoparticles increases the safety considerations required and should only be performed by trained personnel. Prior to each cation exchange reaction, a desired amount of this powder (usually tens of mg) is transferred to a tared septum-capped vial on a calibrated balance. If under- or over-exchange is observed during implementation of either pathway,

the mass of the Cu_{1.8}S nanoparticles should be among the first troubleshooting considerations.

In partial cation exchange reactions using excess metal salt reagents, we found based on empirical observation that a change in particle concentration by a factor of two can have a significant effect on the extent of partial cation exchange, despite the use of a ~40fold molar excess of the exchanging metal relative to the Cu_{1.8}S template. Figure 10A and 10B show the effect of using half (6 mg of Cu_{1.8}S, ~80X excess of Zn²⁺) and double (24 mg of Cu_{1.8}S, ~20X excess of Zn²⁺) the usual 12-mg amount of template nanoparticles when performing a cation exchange reaction of roxbyite Cu_{1.8}S nanorods with Zn²⁺. We find that the general cation exchange behavior is consistent among these different particle concentrations, but the amount of time required to produce the targeted ZnS-Cu_{1.8}S heterostructured nanoparticles is significantly shorter when decreasing the particle concentration to 6 mg. Low Cu_{1.8}S particle concentration results in the formation of multiple cation exchange reaction fronts at early stages of the reaction, followed by rapid conversion to ZnS, resulting in over-exchanged products relative to reactions with higher particle amounts at the same time point. High Cu_{1.8}S particle concentration results in a much more subtle difference in the product ZnS-Cu_{1.8}S heterostructure compared to the "standard" conditions shown in Figure 7. We attribute these different cation exchange behaviors to differences in the density of initial cation exchange nucleation events, which correlate to the available Cu_{1.8}S surface area, which in turns scales with Cu_{1.8}S concentration. These subtle differences may yield irreproducible results and make targeted syntheses challenging, especially if the quantity of roxbyite Cu_{1.8}S is consistently too low. In partial cation exchange reactions using stoichiometrically limited reagents, accurate mass determination is required to calculate the quantity of cation exchange solution to add to the reaction mixture. The mass of Cu_{1.8}S template nanoparticles influence the number of moles of Cu⁺ cations available for exchange with other cations, which ultimately results in under- or over- exchange in the final product if determined incorrectly.

Reaction temperature. Reaction temperature is a critical variable for both cation exchange pathways, as it impacts the reaction rate and the number and/or location of exchanged segments that form within the heterostructured nanoparticle that is produced. If reactions are consistently under- or over- exchanged, or if there are more or fewer exchanged segments, reaction temperature should be considered as a possible reason.

For partial cation exchange reactions using <u>excess</u> metal salt reagents, slight temperature fluctuations of ± 15 °C can significantly impact the extent of cation exchange. For example, in a ZnS–Cu_{1.8}S heterostructure obtained through exchange with <u>excess</u> Zn²⁺, a reaction temperature of 35 °C results in very little conversion to the desired product (Figure 10C), while a reaction temperature of 65 °C causes rapid conversion to ZnS, forming rods that contain very small (> 2 nm) Cu_{1.8}S regions after 90 minutes (Figure 10D). Greatly exceeding the reaction temperature (i.e. 100 °C) decreases the number of exchange regions, resulting in rapid formation of one or two exchanged regions at the tips of the nanorods that quickly propagate through the template, forming nanorods that are almost entirely ZnS within 4 minutes (Figure S4). It is therefore important to strictly

maintain the desired reaction temperature to avoid significant deviations from the intended partial cation exchange behavior.

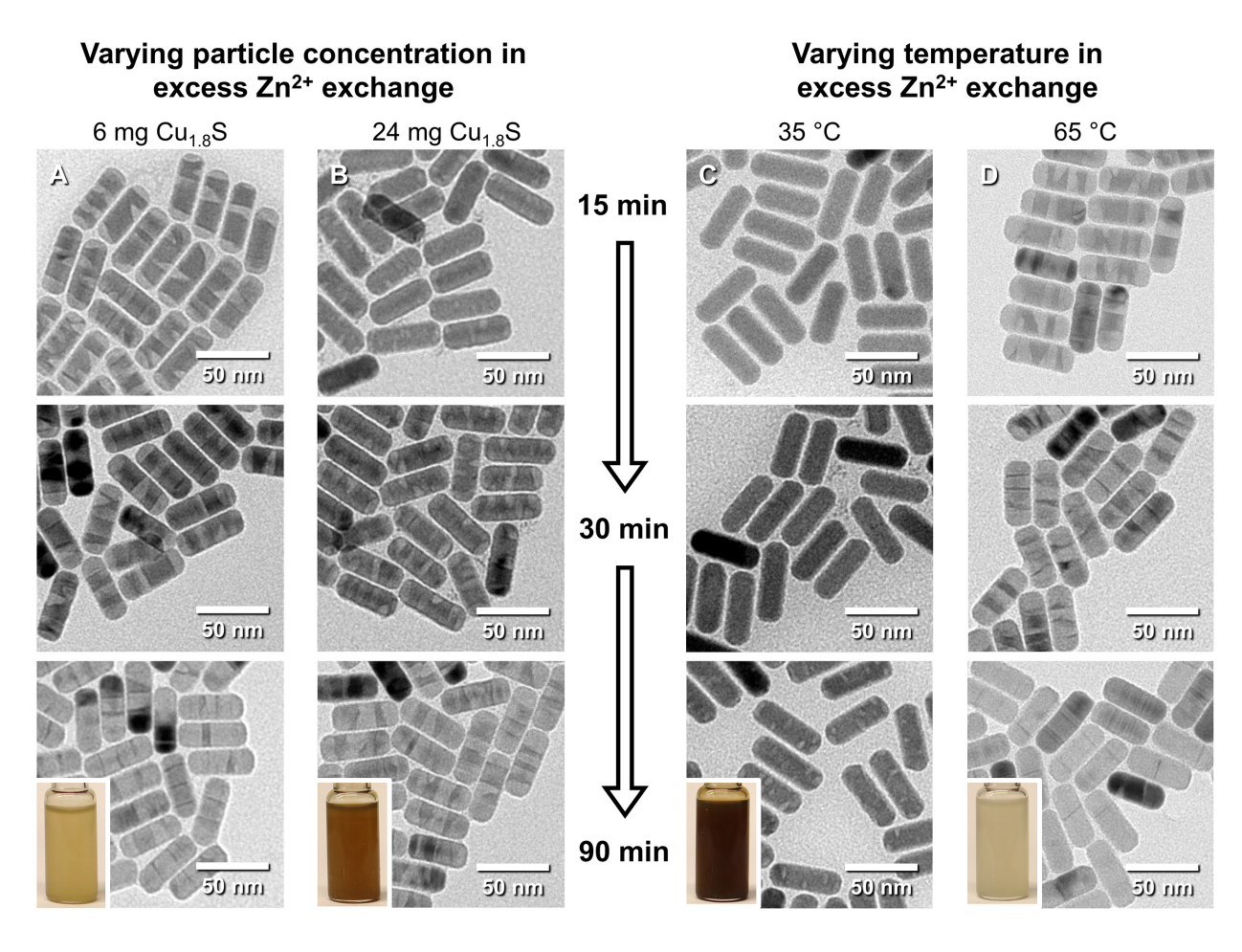


Figure 10. Reaction parameters that affect partial cation exchange using excess metal salt reagents. The data shown are for aliquots removed at 15 minutes (top), 30 minutes (middle), and 90 minutes (bottom) for partial cation exchange of roxbyite Cu_{1.8}S nanorods using excess Zn²⁺. These results can be compared to the data shown in Figure 5, which are representative of the "standard" conditions used for this reaction (12 mg Cu_{1.8}S nanorods, 50 °C reaction temperature) for aliquots removed at each of the same time points. (A) Introducing half of the "standard" quantity of nanorods (6 mg) results in rapid conversion to ZnS and produces ZnS–Cu_{1.8}S nanorods that are consistently over-exchanged at each time point. (B) Introducing double the "standard" quantity of nanorods (24 mg) has a more subtle effect on the reaction outcome and produces ZnS–Cu_{1.8}S nanorods that are very similar to the expected product. (C) Decreasing the reaction temperature to 35 °C results in under-exchanged ZnS–Cu_{1.8}S nanorods with small ZnS domains, even after 90 minutes. (D) Increasing the reaction temperature to 65 °C produces over-exchanged ZnS–Cu_{1.8}S nanorods at each time point and results in nanorods that are almost completely converted to ZnS after 90 minutes. For each 90-minute aliquot, the colors of each nanorod suspension are shown as insets.

For partial cation exchange reactions using <u>stoichiometrically limited</u> reagents, reaction temperature also impacts the product formed from partial cation exchange for the same reasons discussed above when using <u>excess</u> reagents. However, the way

stoichiometrically limited reactions are performed also introduces another significant variable: the injection temperature of the TOP/Cu_{1.8}S suspension. The injection temperature influences the location of the initial partially exchanged region(s),²⁴ and therefore directly impacts the exchange pattern of the heterostructured product. Injecting TOP/Cu_{1.8}S into a cation exchange reaction mixture at or above 120 °C and maintaining this temperature for the entire reaction produces single regions of ZnS at one tip of the Cu_{1.8}S nanorods (ZnS–Cu_{1.8}S). Decreasing the injection and reaction temperature to 90 °C causes multiple exchange regions to form simultaneously in a portion of the nanorods (Figure 11B). These conditions produce a mixture of reaction products, including the ZnS–Cu_{1.8}S nanorods mentioned above as well as nanorods that have ZnS regions at both tips (ZnS–Cu_{1.8}S–ZnS), a single central ZnS band (Cu_{1.8}S–ZnS–Cu_{1.8}S), multiple central ZnS bands, or nearly any combination of these partial exchange patterns.

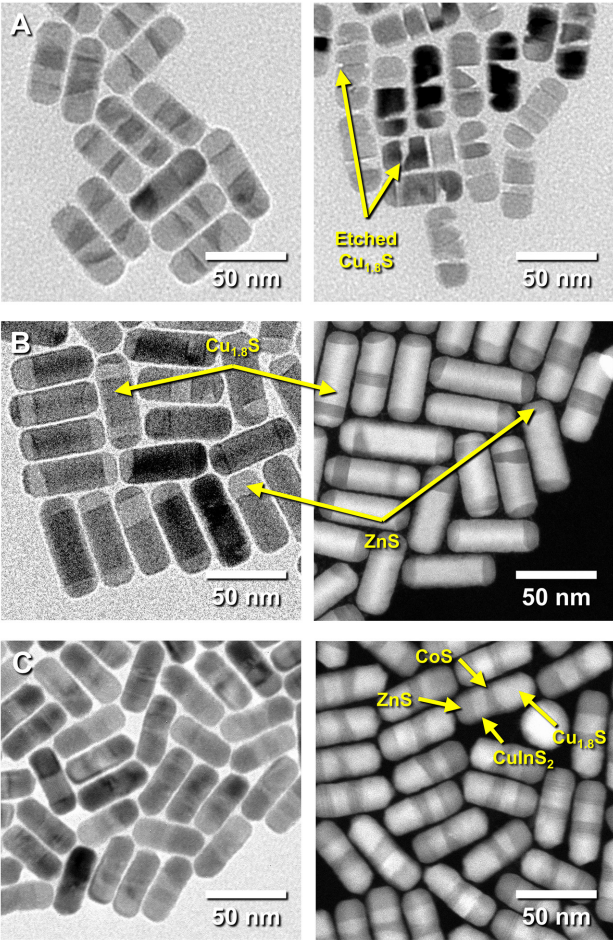


Figure 11. TEM and HAADF-STEM images of selected heterostructured nanorods obtained through partial cation exchange, highlighting common issues encountered during synthesis and characterization. (A, left) If performed correctly, a partial cation exchange reaction with excess Zn²⁺ produces distinct segments of ZnS within the Cu_{1.8}S nanorod. (A, right) If the particle isolation step is performed too slowly or the reaction is cooled insufficiently, the Cu_{1.8}S segments can dissolve due to air exposure, resulting in a product that has etched regions. (B) Bright-field TEM image (left) and HAADF-STEM image (right) of a heterogeneous population of ZnS–Cu_{1.8}S nanorods obtained through stoichiometrically limited partial cation exchange with Zn²⁺ performed at a reaction temperature of 90 °C. The ZnS–Cu_{1.8}S heterostructures contain distinct segments of ZnS and Cu_{1.8}S that can be differentiated using either TEM or HAADF-STEM. (C) Bright-field

TEM image (left) and HAADF-STEM image (right) for ZnS–CuInS₂–CoS–Cu_{1.8}S nanorods obtained through sequential partial cation exchange using stoichiometrically limited metal salt reagents. Segment identification is difficult using TEM, but HAADF-STEM images clearly reveal the various material segments due to increased Z-contrast sensitivity. (A) and (C) are adapted with permission from ref. 24. Copyright 2020 American Association for the Advancement of Science.

Combining these concepts, it is possible to control the outcome of stoichiometrically limited partial cation exchange very precisely. By injecting the TOP/Cu_{1.8}S mixture at room temperature, then ramping the temperature of the reaction flask to 100 °C over 10 minutes (~8 °C/min), Cu_{1.8}S nanorods that almost exclusively contain a central band of ZnS can be produced.²⁴ Using this protocol, exchange can be initiated on the sides of the nanorods at low temperature, then rapidly exchange at only this region during the temperature ramp to 100 °C. Controlling injection temperature and reaction temperature are therefore important for ensuring the highest quality product from each reaction and for precisely targeting a desired heterostructured nanoparticle.

Reaction time. Through empirical observation, long-term exposure of Cu_{1.8}S nanoparticles to elevated temperatures in the presence of TOP and/or oleylamine can result in particle dissolution. The dissolution behavior is attributed to the high affinity for Cu⁺ of both phosphines and amines, the latter of which has been shown to dissolve copper sulfide nanoparticles at room temperature.⁵⁶ It is important to maintain tight control over reaction time and to isolate products from solution as soon as possible. For partial cation exchange reactions using <u>excess</u> metal salt reagents, reaction time is the variable that controls the extent of exchange. Poorly controlling reaction time will lead to widely variable, irreproducible reaction products. For partial cation exchange reactions using <u>stoichiometrically limited</u> reagents, there is likely to be a threshold time required for each reaction to proceed to completion, but the extent of exchange is primarily dictated by the amount of metal salt reagent and the reaction temperature. Thus, these reactions are generally less sensitive to reaction time. For example, we find that 30 minutes at 120 °C is long enough to achieve a high yield of exchange with Zn²⁺, and similar conditions work for many other cation exchange reactions (Table S3).²⁴

Nanoparticle morphology. Trialkylphosphines, such as TOP, have been shown to etch Cu⁺ from copper sulfide when in the presence of an oxidizing agent.³⁷ Although this process can be used in a controlled way, in combination with partial cation exchange, to produce highly intricate products through the selective dissolution of certain regions, ^{23,37} uncontrolled etching of Cu_{1.8}S regions can cause undesired changes in morphology. For this reason, extreme care must be taken to avoid exposure to atmospheric oxygen when performing partial cation exchange reactions, and also to limit exposure to atmosphere when isolating products, if Cu_{1.8}S regions are present.

When the Cu_{1.8}S regions are etched, the product undergoes a subtle color change. For the ZnS–Cu_{1.8}S system, the product color changes from light-brown to white, as expected for a product that contains more ZnS than Cu_{1.8}S. (Figure 6). This color change can be used to qualitatively monitor a reaction to determine if Cu_{1.8}S etching is likely to be occurring. Direct evidence of Cu_{1.8}S etching can be seen in the TEM analysis. The Cu_{1.8}S segments may exhibit significant changes in shape and size relative to the Cu_{1.8}S

template nanoparticles, including thinning or irregular edges, for products that have undergone moderate etching. In cases of severe etching, entire regions of Cu_{1.8}S will dissolve. Depending upon where the Cu_{1.8}S is located in a partially exchanged nanoparticle, TEM images could show notches in certain regions where the Cu_{1.8}S used to be, or fragments that were separated from one another when the Cu_{1.8}S that was joining them was dissolved (Figure 11A).

Two primary steps of the partial cation exchange process most commonly result in the introduction of air. The first occurs during the reaction itself, where air can be introduced when injecting the TOP/Cu_{1.8}S suspension or when withdrawing aliquots. After every step that involves piercing the septum with a needle, it is important to immediately cycle between vacuum and inert gas at least twice to remove any air that may have been introduced. The second occurs during product purification and isolation. Etching during this process is typically a result of inadequate cooling prior to opening the reaction vessel to atmosphere and/or performing the product isolation and purification procedure too slowly. To limit post-reaction etching, ensure that the solution is sufficiently cool (≤ 10 °C) using an ice bath, then promptly transfer it to centrifuge tubes, add the antisolvent, and centrifuge the particles immediately. Centrifuge tubes should be submerged in an ice water bath before moving to and from the centrifuge and subsequent resuspension and centrifugation steps should be performed as quickly as possible.

Particle isolation and centrifugation. The color of the supernatant can provide insights into the particle isolation process in rare cases where particle isolation is a problem. The presence of a cloudy or dark colored supernatant that is similar in color to the expected product nanoparticles likely indicates that nanoparticles are still suspended after centrifugation or that the antisolvent has reacted with residual soluble reagents, i.e. acetone with CoCl₂ exchange solutions, which causes a blue solid to form. If the nanoparticles do not readily precipitate, it can be helpful to add small amounts (1-2 mL) of a more polar antisolvent (typically ethanol or methanol) and/or small amounts (a few drops) of a surfactant.

Characterization of Heterostructured Nanoparticles

As is the case for all nanoparticles, characterization of heterostructured nanoparticles using multiple complementary techniques is important. Various electron microscopy techniques, coupled with bulk-scale diffraction and spectroscopy, provide useful information about particle size, shape, uniformity, elemental composition, crystallinity, and the phases that are present. However, heterostructured nanoparticles have unique characteristics that must be considered when using these techniques.

Preparation of samples for TEM and XRD. Proper sample preparation for the two primary techniques that we use to characterize nanoparticles is required for optimal results. Our commonly used practices for sample preparation, which are based on the approximate volumes and solvents that we typically use for suspending nanoparticle reaction products, are outlined below. To prepare a sample for TEM, we dilute the nanoparticle suspension of interest. We generally transfer a small volume (a few drops to 0.1 mL) of the

nanoparticle suspension to a clean 2-mL microcentrifuge tube. We then add about 1 mL of toluene to the centrifuge tube to produce a colloidal suspension that is optically transparent and very lightly colored. We sonicate this diluted suspension, then using a glass transfer pipet, immediately place one to two drops onto a clean TEM grid. After the solvent has dried completely, the sample is then prepared for TEM analysis. To prepare a sample for XRD, we instead concentrate the nanoparticle suspension. We transfer a moderate volume (~0.5 mL) of our colloidal suspension to a clean 2 mL microcentrifuge tube. We then add about 1 mL of antisolvent (typically isopropyl alcohol) and centrifuge the sample to produce a solid pellet on the bottom of the centrifuge tube. We add a few drops of hexane, then sonicate the centrifuge tube to create a concentrated, dark-colored, colloidal suspension. We then draw the entire contents of the centrifuge tube into a glass transfer pipet and drop cast it onto a clean, zero-background silicon XRD sample holder. After the solvent has dried, there should be a visible film on the silicon. (Note that the sample does not need to cover the entire surface of the zero-background XRD holder) If a film is not visible, repeat the process until one is. Improper sample preparation for either TEM or XRD analysis can complicate data interpretation and make analysis difficult. Table S4 includes some examples of common challenges based on sample preparation that can be encountered for TEM and XRD analysis.

Bright-field transmission electron microscopy (TEM) and scanning TEM (STEM). Initial screening of heterostructured nanoparticle samples by bright-field TEM yields standard information about particle size and shape, and contrast differences within the nanoparticles provide some insight into where the various material components are located due to differences in mass and density.⁵⁷ Bright-field TEM can also easily reveal morphological changes that may occur during partial cation exchange reactions, as well as the presence and location of etched regions that form from the dissolution of Cu_{1.8}S regions (Figure 11A). However, crystal orientation and internal strain can also contribute to contrast differences between and within particles. These factors, combined with the knowledge that materials having similar compositions will have similar contrast, make bright-field TEM insufficient for analyzing heterostructured nanoparticles, particularly those that contain more than two different kinds of metal sulfide materials. STEM images collected using a high-angle, annular dark-field detector (HAADF), i.e. HAADF-STEM, is more sensitive to atomic number (i.e. Z-contrast) than bright field TEM and can mitigate or eliminate diffractive contrast that is common in bright field TEM.⁵⁸ Figure 11 shows several examples where bright-field TEM can be used to analyze partial cation exchange products, as well as systems where HAADF-STEM is more useful due to the aforementioned reasons. In ZnS-Cu_{1.8}S heterostructures, for example, the ZnS and Cu_{1.8}S regions can be differentiated using both bright-field TEM and HAADF-STEM (Figure 11B). However, heterostructures containing a larger number of materials, such as the ZnS-CuInS2-CoS-Cu1.8S nanorods in Figure 11C, require HAADF-STEM to unambiguously differentiate the various segments within the heterostructure. In general, bright-field TEM is easier to perform and can be used to identify morphological features and exchange behavior in certain systems, while HAADF-STEM can be more difficult, but can provide additional information in heterostructured systems. Commonly these techniques are used together when characterizing heterostructured metal chalcogenide nanoparticles, but neither alone is sufficient. Bright-field TEM and HAADF-STEM alone

do not explicitly give compositional or elemental information. Additionally, the contrast differences between material segments that have mean atomic numbers that are the same or similar are difficult to discern. Therefore, these techniques should be used in conjunction with a technique that yields spatially resolved elemental information to confidently assign material identity.

STEM with energy dispersive spectroscopy (STEM-EDS). EDS is often used in conjunction with HAADF-STEM imaging to produce element maps that reveal where specific elements are located within heterostructured nanoparticles. EDS element maps can be collected for a large group of nanoparticles, a small group of particles, or a single particle, with different resolutions in each case – higher-resolution images, and therefore higher resolution EDS maps, are produced using higher-magnification data (Figure S5). EDS spectra for specific regions of the heterostructures can be collected using a 0D point scan, a 1D line scan, or a 2D map.³⁴ Semi-quantitative analysis can be performed to determine the relative ratios of selected elements. It is worth noting that such EDS analyses have errors in measurement based on several factors, including the identity of the element analyzed and the number of counts.⁵⁹ Errors when using low-intensity and/or overlapping X-ray emission lines can be more significant. Signals for the highest-intensity X-ray emission lines of certain elements, such as Cd and In, overlap significantly, which can pose significant problems during data analysis. For example, it will erroneously appear as if In is present in the Cd region due to overlap of the most commonly mapped In Lα line (3.286 keV) with the Cd Lβ (3.315 keV) line, as shown in the ZnS-CuInS₂-CuGaS2-CoS-(CdS-Cu_{1.8}S) nanorod in Figure 12A. By instead using the weaker, but non-overlapping In Kα line at 24.210 keV, the two elements can be differentiated, as shown for the same nanorod in Figure 12B. It is therefore important to analyze the ensemble EDS spectrum for a representative portion of each sample to ensure that signal is significantly above baseline for the expected elements and that overlapping signal(s) are not used. Note that it can be possible to deconvolute the signal for overlapping elements through data profile fitting, such as a quantitative map (QMAP) using the Bruker Espirit II software package. Other TEM-based techniques, such as electron energy loss spectroscopy (EELS) and energy filtered (EF)-TEM, can be used to obtain elemental information from similar nanoscale materials and each has their own advantages and disadvantages. 59,60 For all systems that we have investigated to date, STEM-EDS has provided sufficient information to identify the composition of each material segment, even in complex, multicomponent heterostructures.^{23,34,27}

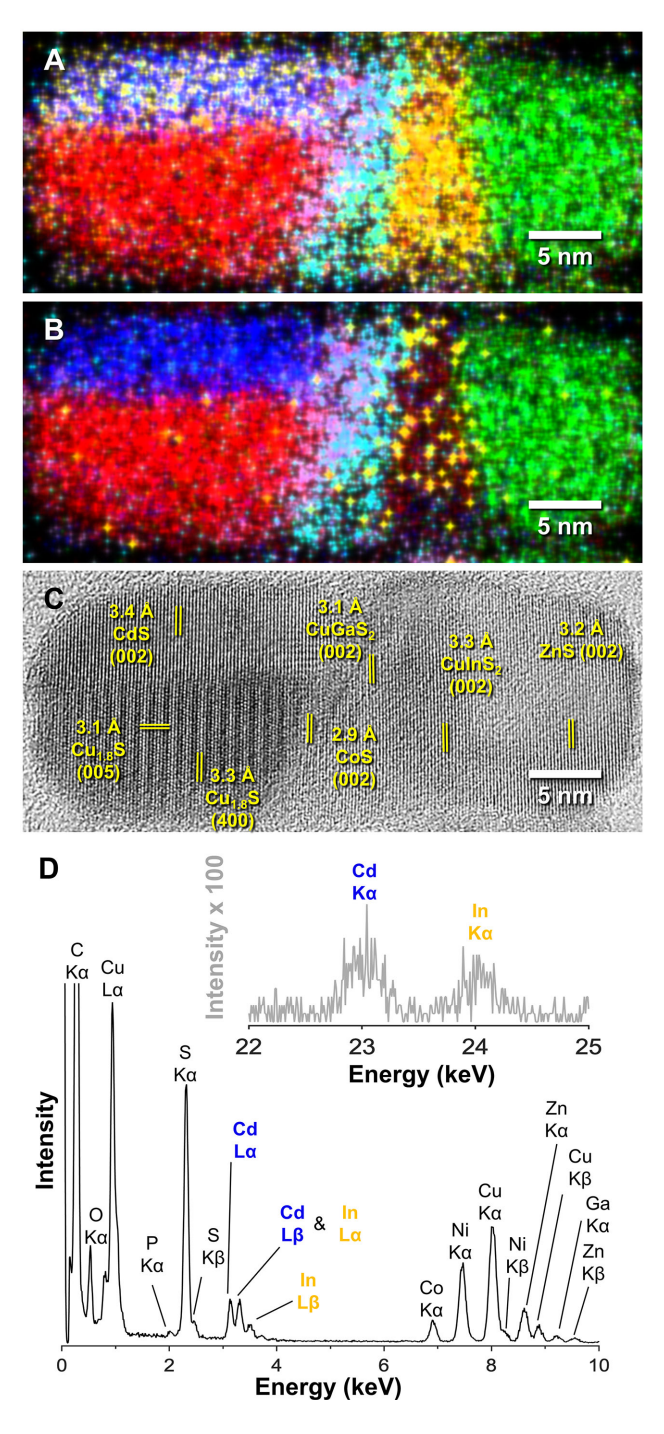


Figure 12. STEM-EDS and HRTEM characterization of ZnS–CulnS₂–CuGaS₂–CoS–(CdS–Cu_{1.8}S) nanorods obtained through sequential partial cation exchange using stoichiometrically limited metal salt reagents. (A) STEM-EDS element map generated by selecting to map the ln Lα line, which overlaps strongly with the Cd Lβ line, compared to (B) a STEM-EDS element map of the same nanorod using the non-overlapping ln Kα line. Cu Kα, Zn Kα, ln Kα, Ga Kα, Co Kα, and Cd Lα lines are shown in red, green, yellow, teal, purple, and blue, respectively. (C) HRTEM image with lattice fringe assignments of the same nanorod in (A) and (B). Identification of regions within the heterostructured nanorod were assigned based on analysis of the STEM-EDS element maps. (D) Ensemble EDS spectrum of dozens of ZnS–CulnS₂–CuGaS₂–CoS–(CdS–Cu_{1.8}S) heterostructured nanorods showing the assignments of each signal present in the sample. Note the overlap of the ln Lα and Cd Lβ lines. The inset shows that the ln Kα line does not

overlap the Cd K α line but is significantly lower in signal. Adapted with permission from ref. 24. Copyright 2020 American Association for the Advancement of Science.

High-resolution TEM (HRTEM). HRTEM allows for imaging of lattice fringes and/or columns of atoms within a crystalline material. Two or three types of different material segments can usually be identified and differentiated in heterostructured nanoparticles using HRTEM.^{22,23,26,27} However, HRTEM is inherently a bright-field imaging technique and therefore has similar limitations as low-resolution bright-field TEM. D-spacings, which differ slightly for many different metal sulfides phases, can be determined from HRTEM, but the measurements possible by even a well-aligned microscope are often not precise enough to distinguish between metal sulfide regions with different compositions. HRTEM can offer useful complementary information when coupled with STEM-EDS on the same particle(s), as shown in Figure 12C for the same ZnS–CuInS₂–CuGaS₂–CoS–(CdS–Cu_{1.8}S) nanorod shown in Figure 12 A and B.

Selected area electron diffraction (SAED). SAED patterns provide useful structural information for nanoparticle samples. However, cation exchange reactions on metal sulfide nanoparticles generally preserves crystal structure, and partial cation exchange typically produces heterostructured nanoparticles with material segments having the same crystal structure. For example, all segments of the ZnS–CuInS₂–CuGaS₂–CoS–(CdS–Cu_{1.8}S) nanorod shown in Figure 12 have the wurtzite structure. Different materials that have the same crystal structure, but slightly different lattice parameters (as is the case for most the metal sulfides discussed herein), will exhibit only slight radial shifts in the observed diffraction rings, and therefore does not generally allow unambiguous phase identification.

Powder X-ray diffraction (XRD). XRD provides useful and important structural information involving material phase, particle shape and size, crystallinity, and purity for bulk-scale samples, thereby complementing the microscopic characterization and confirming that what is observed microscopically is representative of the bulk. 61 The diffraction patterns obtained for products obtained through partial cation exchange have broad peaks due to small crystallite sizes. When performing partial exchange on roxbyite Cu_{1.8}S nanorods, the products all adopt a wurtzite-type crystal structure. Broad peaks that are similarly spaced can be challenging to analyze but can be deconvoluted to determine which phases are present, as well as their phase fractions. Figure 13A shows the similarities between simulated diffraction patterns for roxbyite Cu_{1.8}S and five common wurtzite-type products obtained from partial cation exchange – ZnS, CuInS₂, CuGaS₂, CoS, and CdS - with crystallite sizes of 15 nm. Empirical adjustment of lattice parameters and phase fractions, use of average crystallite sizes for each material as obtained by TEM analysis, and adjustment for preferred orientation due to the nanorod shape produces a combined simulated XRD pattern that matches well with the experimental data, as shown in Figure 13B. These data show how good agreement between an experimental XRD pattern and a simulated multi-component XRD pattern can provide validation that heterostructured nanoparticles observed microscopically are representative of the bulk.

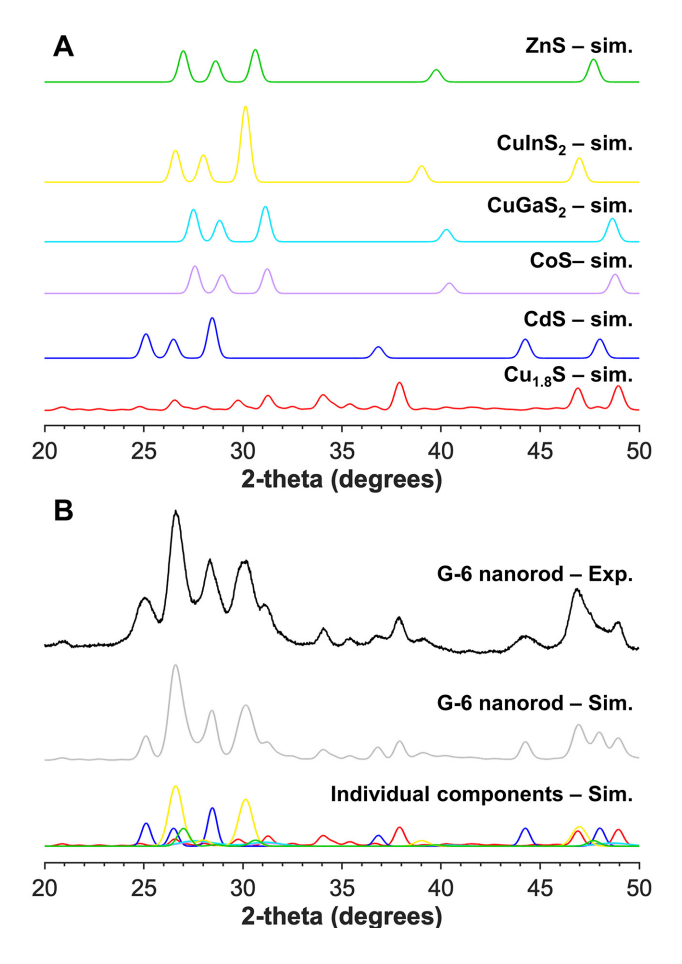


Figure 13. XRD analysis of heterostructured nanorods obtained through sequential partial cation exchange using stoichiometrically limited metal salt reagents. (A) Simulated diffraction patterns of roxbyite Cu_{1.8}s and five wurtzite-type materials that can be obtained through cation exchange. Each simulated pattern has a crystallite size of 15 nm, which results in peak broadening. (B) Experimental and simulated diffraction patterns for ZnS–CuInS₂–CuGaS₂–CoS–(CdS–Cu_{1.8}S) nanorods. The simulated pattern was obtained by assigning crystallite sizes, preferred orientation effects, and phase fraction of each material based on TEM analysis. Lattice parameters were empirically adjusted based on known variances for certain phases (i.e. due to slight stoichiometry differences). (B) was adapted with permission from ref. 24. Copyright 2020 American Association for the Advancement of Science.

Conclusions

Partial cation exchange is a powerful and versatile strategy that can be used to rationally synthesize complex heterostructured nanoparticles. Two methods, which are related but distinct, can be used: partial cation exchange reactions using <u>excess</u> metal salt reagents and partial cation exchange reactions using <u>stoichiometrically limited</u> reagents. Cation exchange behavior can vary significantly between these two methods and both are sensitive to subtle changes in the reaction parameters. Careful consideration of synthetic methodology, characterization requirements, and relevant physical and chemical hazards are important for successful and safe implementation. Being aware of, and understanding, the most common ways in which the reactions can fail to produce desired

products is helpful for troubleshooting and achieving reproducibility. Applying these procedures and experimental insights to new and more complex systems will further expand the scope and applicability of synthetically accessible heterostructured nanoparticles.

ASSOCIATED CONTENT

Supporting Information. Photos of reaction setup, part numbers of common equipment used, preparation of exchange solutions, reagent quantities, reaction conditions, characterization considerations, and a troubleshooting table. This material is available free of charge via the Internet at http://pubs.acs.org.

AUTHOR INFORMATION

Corresponding Author

* R. E. Schaak. Email: res20@psu.edu

Notes

The authors declare no competing financial interest.

ACKNOWLEDGMENT

This work was supported by the U.S. National Science Foundation under grant DMR-1904122.TEM/STEM imaging and EDS mapping were performed at the Materials Characterization Laboratory of the Penn State Materials Research Institute.

References

- 1. Xie, R.; Kolb, U.; Li, J. Basché, T.; Mews, A. Synthesis and Characterization of Highly Luminescent CdSe-Core CdS/Zn_{0.5}Cd_{0.5}S/ZnS Multishell Nanocrystals. *J. Am. Chem. Soc.* **2005**, 127, 7480-7488.
- 2. Enright, M. J.; Cossairt, B. M. Synthesis of Tailor-Made Colloidal Semiconductor Heterostructures. *Chem Commun.* **2018**, 54, 7109-7122.
- 3. Sitt, A.; Hadar, I.; Banin, U. Band-Gap Engineering, Optoelectronic Properties and Applications of Colloidal Heterostructured Semiconductor Nanorods. *Nano Today.* **2013**, 8, 494-513.
- 4. Zhuang, T.-T.; Liu, Y.; Li, Y.; Zhao, Y.; Liang, W.; Jiang, J.; Yu, S.-H. Integration of Semiconducting Sulfides for Full-Spectrum Solar Energy Adsorption and Efficient Charge Separation. *Angew. Chem. Int. Ed.* **2016**, 55, 6396-6400.
- 5. Chandrasekaran, S.; Yao, L.; Deng, L.; Bowen, C.; Zhang, Y.; Chen, S.; Lin, Z.; Peng, F.; Zhang, P. Recent Advances in Metal Sulfides: From Controlled Fabrication to

- Electrocatalytic, Photocatalytic, and Photoelectrochemical Water Splitting and Beyond. *Chem. Soc. Rev.* **2019**, 48, 4178-4280.
- 6. Oh, N.; Kim, B. H.; Cho, S.-Y.; Nam, S.; Rogers, S. P.; Jiang, Y.; Flanagan, J. C.; Zhai, Y.; Kim, J.-H., Lee, J.; Yu, Y.; Cho, Y. K.; Hur, G.; Zhang, J.; Trefonas, P.; Rogers, J. A.; Shim, M. Double-Heterojunction Nanorod Light-Responsive LEDs for Display Applications. *Science* **2017**, 355, 616-619.
- 7. Panfil, Y. E.; Oded, M.; Banin, U. Colloidal Quantum Nanostructures: Emerging Materials for Display Applications. *Angew. Chem. Int. Ed.* **2018**, 57, 4274-4295.
- 8. Min, Y.; Park, G.; Kim, B.; Giri, A.; Zeng, J.; Roh, J. W.; Kim, S. I.; Lee, K. H.; Jeong, U. Synthesis of Multishell Nanoplates by Consecutive Epitaxial Growth of Bi₂Se₃ and Bi₂Te₃ Nanoplates and Enhanced Thermoelectric Properties. *ACS Nano* **2015**, 9, 6843-6853.
- 9. Costi, R.; Saunders, A. E.; Banin, U. Colloidal Hybrid Nanostructures: A New Type of Functional Materials. *Angew. Chem. Int. Ed.* **2010**, 49, 4878-4897.
- 10. Hodges, J. M.; Schaak, R. E. Controlling Configurational Isomerism in Three-Component Colloidal Hybrid Nanoparticles. *Acc. Chem. Res.* **2017**, 50, 1433-1440.
- 11. Buck, M. R.; Schaak, R. E. Emerging Strategies for the Total Synthesis of Inorganic Nanostructures. *Angew. Chem. Int. Ed.* **2013**, 52, 6154-6178.
- 12. Beberwyck, B. J.; Surendranath, Y.; Alivisatos, A. P. Cation Exchange: A Versatile Tool for Nanomaterials Synthesis. *J. Phys. Chem. C* **2013**, 117, 19759-19770.
- 13. Rivest, J. B.; Jain, P. K. Cation Exchange on the Nanoscale: An Emerging Technique for New Material Synthesis, Device Fabrication, and Chemical Sensing. *Chem. Soc. Rev.* **2013**, 42, 89-96.
- 14. De Trizio, L.; Manna, L. Forging Colloidal Nanostructures via Cation Exchange Reactions. *Chem. Rev.* **2016**, 116, 10852-10887.
- 15. Son, D. H.; Hughes, S. M.; Yin, Y.; Alivisatos, A. P.; Cation Exchange Reactions in Ionic Nanocrystals. *Science* **2004**, 306, 1009-1012.
- 16. Luther, J. M.; Zheng, H.; Sadtler, B.; Alivisatos, A. P.; Synthesis of PbS Nanorods and Other Ionic Nanocrystals of Complex Morphology by Sequential Cation Exchange Reactions. *J. Am. Chem. Soc.* **2009**, 131, 16851-16857.
- 17. Li, H.; Zanella, M.; Genovese, A.; Povia, M.; Falqui, A.; Giannini, C.; Manna, L. Sequential Cation Exchange in Nanocrystals: Preservation of Crystal Phase and Formation of Metastable Phases. *Nano Lett.* **2011**, 11, 4964-4970.
- 18. Jain, P. K.; Amirav, L.; Aloni, S.; Alivisatos, A. P.; Nanoheterostructure Cation Exchange: Anionic Framework Conservation. *J. Am. Chem. Soc.* **2010**, 132, 9997-9999.
- 19. Fenton, J. L.; Schaak, R. E. Structure-Selective Cation Exchange in the Synthesis of Zincblende MnS and CoS Nanocrystals. *Angew. Chem. Int. Ed.* **2017**, 56, 6464-6467.

- 20. Fenton, J. L.; Steimle, B. C.; Schaak, R. E.; Structure-Selective Synthesis of Wurtzite and Zincblende ZnS, CdS, and CuInS₂ Using Nanoparticle Cation Exchange Reactions. *Inorg. Chem.* **2019**, 58, 672-678.
- 21. Powell, A. E.; Hodges, J. M.; Schaak, R. E. Preserving Both Anion and Cation Sublattice Features During a Nanocrystal Cation-Exchange Reaction: Synthesis of Metastable Wurtzite-Type CoS and MnS. *J. Am. Chem. Soc.* **2016**, 138, 471-474.
- 22. Liu, Y.; Liu, M.; Yin, D.; Qiao, L.; Fu, Z.; Swihart, M. T. Selective Cation Incorporation into Copper Sulfide Based Nanoheterostructures. *ACS Nano* **2018**, 12, 7803-7811.
- 23. Fenton, J. L.; Steimle, B. C.; Schaak, R. E. Tunable Intraparticle Frameworks for Creating Complex Heterostructured Nanoparticle Libraries. *Science* **2018**, 360, 513-517.
- 24. Steimle, B. C.; Fenton, J. L.; Schaak, R. E. Rational Construction of a Scalable Heterostructured Nanorod Megalibrary. *Science* **2020**, 367, 418-424.
- 25. Ha, D.-H.; Caldwell, A. H.; Ward, M. J.; Honrao, S.; Mathew, K.; Hovden, R.; Koker, M. K. A.; Muller, D. A.; Henning, R. G.; Robinson, R. D. Solid-Solid Phase Transformations Induced through Cation Exchange and Strain in 2D Heterostructured Copper Sulfide Nanocrystals. *Nano Lett.* **2014**, 14, 7090-7099.
- 26. Sadtler, B.; Demchenko, D. O.; Zheng, H.; Hughes, S. M.; Merkle, M. G.; Dahmen, U.; Wang, L.-W., Alivisatos, A. P. Selective Facet Reactivity During Cation Exchange in Cadmium Sulfide Nanorods. *J. Am. Chem. Soc.* **2009**, 131, 5285-5293.
- 27. Fenton, J. L.; Steimle, B. C.; Schaak, R. E. Exploiting Crystallographic Regioselectivity To Engineer Asymmetric Three-Component Colloidal Nanoparticle Isomers Using Partial Cation Exchange Reactions. *J. Am. Chem. Soc.* **2018**, 140, 6771-6775.
- 28. Gui, J.; Ji, M.; Liu, J.; Xu, M.; Zhang, J.; Zhu, H. Phosphine-Initiated Cation Exchange for Precisely Tailoring Composition and Properties of Semiconductor Nanostructures: Old Concept, New Applications. *Angew. Chem. Int. Ed.* **2015**, 54, 3683-3687.
- 29. Coughlan, C.; Ibáñez, M.; Dobrozhan, O.; Singh, A.; Cabot, A.; Ryan, K. M. Compound Copper Chalcogenide Nanocrystals. *Chem. Rev.* **2017**, 117, 5865-6109.
- 30. Mumme, W. G.; Gable, R. W.; Petříček, V. The Crystal Structure of Roxbyite, Cu₅₈S₃₂. *The Canadian Mineralogist* **2012**, 50, 423-430.
- 31. Park, J.; Park, J.; Lee, J.; Oh, A.; Baik, H.; Lee, K. Janus Nanoparticle Structural Motif Control via Asymmetric Cation Exchange in Edge-Protected Cu_{1.81}S@Ir_xS_y Hexagonal Nanoplates. *ACS Nano* **2018**, 12, 7996-8005.
- 32. Tan, J. M. R.; Scott, M. C.; Hao, W.; Baikie, T.; Nelson, C. T.; Pedireddy, S.; Tao, R; Ling, X.; Magdassi, S.; White, T.; Li, S.; Minor, A. M.; Zheng, H.; Wong, L. H. Revealing Cation-Exchange-Induced Phase Transformations in Multielemental Chalcogenide Nanoparticles. *Chem. Mater.* **2017**, 29, 9192-9199.
- 33. Park, J.; Jin, H.; Lee, J.; Oh, A.; Kim, B.; Kim, J. H.; Baik, H.; Joo, S. H.; Lee, K. Highly Crystalline Pd₁₃Cu₃S₇ Nanoplates Prepared via Partial Cation Exchange of Cu_{1.81}S

- Templates as an Efficient Electrocatalyst for the Hydrogen Evolution Reaction. *Chem. Mater.* **2018**, 30, 6884-6892.
- 34. Hodges, J. M.; Morse, J. R.; Fenton, J. L.; Ackerman, J. D.; Alameda, L. T.; Schaak, R. E. Insights into the Seeded-Growth Synthesis of Colloidal Hybrid Nanoparticles. *Chem. Mater.* **2017**, 29, 106-119.
- 35. Borys, A. The Schlenk Line Survival Guide. https://schlenklinesurvivalguide.com (accessed March 31, 2020).
- 36. Chandra, T.; Zebrowski, J. P. Reactivity Control using a Schlenk Line. *J. Chem. Health Saf.* **2014**, 21, 22-28.
- 37. Nelson, A.; Ha, D.-H.; Robinson, R. D. Selective Etching of Copper Sulfide Nanoparticles and Heterostructures through Sulfur Abstraction: Phase Transformations an Optical Properties. *Chem. Mater.* **2016**, 28, 8530-8541.
- 38. Groso, A.; Petri-Fink, A.; Magrez, A.; Riediker, M.; Meyer, T. Management of Nanomaterials Safety in Research Environment. *Part. Fibre Toxicol.* **2010**, 7, 1-8.
- 39. Groso, A.; Petri-Fink, A.; Rothen-Rutishauser, B.; Hofmann, H.; Meyer, T. Engineered Nanomaterials: Toward Effective Safety Management in Research Laboratories. *J. Nanobiotechnol.* **2016**, 21, 1-17.
- 40. Beaucham, C.; Hodson, L. General Safe Practices for Working with Engineered Nanomaterials in Research Laboratories; DHHS (NIOSH) Publication No. 212-147; Department of Health and Human Services, Centers for Disease Control and Prevention, National Institute for Occupational Safety and Health: 2012
- 41. Zumwalde, R.; Hodson, L. *Approaches to Safe Nanotechnology: Managing the Health and Safety Concerns Associated with Engineered Nanomaterials*; DHHS (NIOSH) Publication No. 2009-125; Department of Health and Human Services, Centers for Disease Control and Prevention, National Institute for Occupational Safety and Health: **2009**.
- 42. Buzea, C.; Pacheco, I. I.; Robbie, K. Nanomaterials and Nanoparticles: Sources and Toxicity. *Biointerphases.* **2007**, 2, MR17-MR71.
- 43. Wang, F.; Tang, R.; Buhro, W. E. The Trouble with TOPO; Identification of Adventitious Impurities Beneficial to the Growth of Cadmium Selenide Quantum Dots, Rods, and Wires. *Nano Lett.* **2008**, 8, 3521-3524.
- 44. Hughes, B. K.; Luther, J. M.; Beard, M. C. The Subtle Chemistry of Colloidal, Quantum-Confined Semiconductor Nanostructures. *ACS Nano* **2012**, 6, 4573-4579.
- 45. Buck, M. R.; Biacchi, A. J.; Schaak, R. E. Insights into the Thermal Decomposition of Co(II) Oleate for the Shape-Controlled Synthesis of Wurtzite-Type CoO Nanocrystals. *Chem. Mater.* **2014**, 26, 1492-1499.
- 46. Bronstein, L. M.; Huang, X.; Retrum, J.; Schmucker, A.; Pink, M.; Stein, B. D.; Dragnea, B. Influence of Iron Oleate Complex Structure on Iron Oxide Nanoparticle Formation. *Chem. Mater.* **2007**, 19, 3624-3632.

- 47. Qiao, L.; Fu, Z.; Ghosen, J.; Zeng, M.; Stebbins, J.; Prasad, P. N.; Swihart, M. T. Standardizing Size- and Shape-Controlled Synthesis of Monodisperse Magnetite (Fe₃O₄) Nanocrystals by Identifying and Exploiting Effects of Organic Impurities. *ACS Nano* **2017**, 11, 6370-6381.
- 48. Dhaene, E.; Billet, J.; Bennett, E.; Van Driessche, I.; De Roo, J. The Trouble with ODE: Polymerization during Nanocrystal Synthesis. *Nano Lett.* **2019**, 19, 7411-7417.
- 49. Mourdikoudis, S.; Liz-Marzán, L. M. Oleylamine in Nanoparticle Synthesis. *Chem. Mater.* **2013**, 25, 1465-1476.
- 50. Baranov, D.; Lynch, M. J.; Curtis, A. C.; Carollo, A. R.; Douglass, C. R.; Mateo-Tejada, A. M.; Jonas, D. M. Purification of Oleylamine for Material Synthesis and Spectroscopic Diagnostics for *trans* Isomers. *Chem. Mater.* **2019**, 31, 1223-1230.
- 51. Zhai, Y.; Shim, M. Effects of Copper Precursor Reactivity on the Shape and Phase of Copper Sulfide Nanocrystals. *Chem. Mater.* **2017**, 29, 2390-2397.
- 52. Kruszynska, M.; Borchert, H.; Bachmatiuk, A.; Rümmeli, M. H.; Büchner, B.; Parisi, J.; Kolny-Olesiak, J. Size and Shape Control of Colloidal Copper(I) Sulfide Nanorods. *ACS Nano* **2012**, 6, 5889-5896.
- 53. Ding, X.; Zou, Y.; Jiang, J. Au-Cu₂S Heterodimer Formation via Oxidation of AuCu Alloy Nanoparticles and In Situ formed Copper Thiolate. *J. Mater. Chem.* **2012**, 22, 23169-23174.
- 54. Zhai, Y.; Shim, M. Cu₂S/ZnS Heterostructured Nanorods: Cation Exchange vs. Solution-Liquid-Solid-like Growth. *ChemPhysChem* **2016**, 17, 741-751.
- 55. Robinson, R. D.; Sadtler, B.; Demchenko, D. O.; Erdonmez, C. K.; Wang, L.-W.; Alivisatos, A. P. Spontaneous Superlattice Formation in Nanorods Through Partial Cation Exchange. *Science* **2007**, 317, 355-358.
- 56. Liu, L.; Zhong, H.; Bai, Z.; Zhang, T.; Fu, W.; Shi, L.; Xie, H.; Deng, L.; Zou, B. Controllable Transformation from Rhombohedral Cu_{1.8}S Nanocrystals to Hexagonal CuS Clusters: Phase- and Composition-Dependent Plasmonic Properties. *Chem. Mater.* **2013**, 25, 4828-4834.
- 57. Williams, D. B.; Carter, C. B. *Transmission Electron Microscopy: A Textbook for Materials Science*; Springer: Boston, MA, 2009.
- 58. Pennycook, S. J. In *Electron Microscopy: Diffraction, Imaging, and Spectrometry*; Carter, B., Williams, D. B., Eds.; Springer: Cham, Switzerland, 2016; Chapter 11, pp 283–342.
- 59. Kotula, P. In *Electron Microscopy: Diffraction, Imaging, and Spectrometry*; Carter, B., Williams, D. B., Eds.; Springer: Cham, Switzerland, 2016; Chapter 16, pp 439–466.
- 60. Thomas, P.; Midgley, P. In *Electron Microscopy: Diffraction, Imaging, and Spectrometry*; Carter, B., Williams, D. B., Eds.; Springer: Cham, Switzerland, 2016; Chapter 13, pp 377–404.

61. Holder, C. F.; Schaak, R. E. Tutorial on Powder X-Ray Diffraction for Characterizing Nanoscale Materials. *ACS Nano* **2019**, 13, 7359-7365.

Table of Contents (TOC) Graphic

